GEORGIA INSTITUTE OF TECHNOLOGY
OFFICE OF RESEARCH ADMINISTRATION

RESEARCH PROJECT INITIATION

Date: November 20, 1973

Project Title: Investigation of Field Emission Electron Guns for Gas Lasers

Project No: E-18-606 and E-21-636

Principal Investigator: Dr. A. T. Chapman & Dr. R. K. Feeney

Sponsor: U. S. Army Missile Command; Redstone Arsenal, Alabama

Agreement Period: From 10/12/73 Until 10/11/74

Type Agreement: Contract No. DAAH01-74-C-0229

Amount: $55,458 ($32,323 for E-18-606 & $23,135 for E-21-636)

Reports Required: Quarterly Progress Letters; Final Technical Report

Sponsor Contact Person (s):

Technical Matters	Contractual Matters
(Individual not specified) U. S. Army Missile Command ATTN: AMSMI-RR Redstone Arsenal, Alabama 35809	(Thru ORA) Mr. R. J. Whitcomb (ACO) ONRR Campus

Defense Priority Rating: DO-A2 under DMS Reg. 1.

Assigned to: Cer. Eng./ EE

COPIES TO:

Principal Investigator	Library
School Director	Rich Electronic Computer Center
Dean of the College	Photographic Laboratory
Director, Research Administration	Project File
Director, Financial Affairs (2)	
Security-Reports-Property Office ✓	
Patent Coordinator	Other

RA-3 (6-71)

GEORGIA INSTITUTE OF TECHNOLOGY
OFFICE OF CONTRACT ADMINISTRATION

SPONSORED PROJECT TERMINATION

Date: September 9, 1976

Project Title: Investigation of Field Emission Electron Guns for Gas Lasers

Project No: E-18-606/E-21-636

Project Director: Dr. A. T. Chapman & Dr. R. K. Feeney

Sponsor: U. S. Army Missile Command; Redstone Arsenal, Alabama

Effective Termination Date: 8/31/75

Clearance of Accounting Charges: All have cleared.

Grant/Contract Closeout Actions Remaining: None

- _ Final Invoice and Closing Documents
- _ Final Fiscal Report
- _ Final Report of Inventions
- _ Govt. Property Inventory & Related Certificate
- _ Classified Material Certificate
- _ Other _____

Assigned to: Ceramic Engineering/Electrical Engineering (School/Laboratory)

COPIES TO:

Project Director
Division Chief (EES)
School/Laboratory Director
Dean/Director—EES
Accounting Office
Procurement Office
Security Coordinator (OCA)
Reports Coordinator (OCA)
Library, Technical Reports Section
Office of Computing Services
Director, Physical Plant
EES Information Office
Project File (OCA)
Project Code (GTRI)
Other _____

CA—4 (3/76)

QUARTERLY PROGRESS LETTER

13 October 1973 - 11 January 1974

INVESTIGATION OF FIELD EMISSION ELECTRON GUNS FOR GAS LASERS

U. S. Army Missile Command

Contract No. DAAH01-74-C-0229

School of Electrical Engineering
Georgia Institute of Technology
Atlanta, Georgia 30332

QUARTERLY PROGRESS LETTER

on

INVESTIGATION OF FIELD EMISSION ELECTRON GUNS FOR GAS LASERS

Contract No. DAAH01-74-C-0229

This is the first Quarterly Progress Letter which, covers the period from 13 October 1973 to 11 January 1974.

Upon completion of an initial technical conference with Mr. Cason and his associates at the U. S. Army Missile Command, detailed design work was begun on the required test apparatus and fixtures. Drawings for the experimental vacuum tubes were sent to three vendors. At this time two of the three vendors have "no bid" the order. If the remaining vendor is unable to supply the needed tubes, they will be produced at Georgia Tech using an alternative design. Preliminary tests can be made using existing glass/metal tube designs.

A rf induction heater previously ordered has arrived and is undergoing installation. This apparatus will be used to thoroughly outgas test diode components in situ at temperatures of 1000^{o} C and above.

As part of a continuing program to improve the performance of the oxide-metal composite field emitters, a sample having a small number of pins ($\sim$ 500) was prepared. This sample was installed in the test diode and after bakeout was subjected to electrical measurements. A large (7 megohm) resistance was inserted in series with the wafer and the anode voltage increased from zero until emission was observed. Emission was slowly increased over about a 48 hour period until a current density of about 5×10^{-4} A/cm^2 was obtained. Stability of emission current was approximately $\pm$ 20%. After operation for about 48 additional hours the

stability improved to ± 10%. At this point it was decided to strive for maximum current density, and a current density of 5 A/cm^2 was achieved with about 5 kV applied to the diode. The water cooling capability of the diode was activated at this time. Operation at the 5 A/cm^2 current level was continued for about 48 hours after which the current was increased to nearly 20 A/cm^2. The current remained relatively constant at this value with short term fluctuations of about ± 10% for 48 hours after which it began to decrease. After three days the current density had decayed 50% and after 5 days to about 10%.

The emission current density observed in these tests was the largest ever obtained from the oxide-metal composites. The fact that these densities were obtained with a small emitter area, and attendant low total anode bombardment is perhaps indicative that anode-initiated destruction mechanisms are of more importance than previously believed.

It is planned to continue with the design and construction of the necessary experimental tubes and associated high-voltage test fixtures. Concurrently, samples having desirable growth characteristics will be prepared for installation in the emission test facility. A modest theoretical effort devoted to the prediction of emitter/marx generator transient behavior will continue.

E-18-606 / E-21-6

QUARTERLY PROGRESS LETTER

12 January 1974 - 11 April 1974

INVESTIGATION OF FIELD EMISSION ELECTRON GUNS FOR GAS LASERS

U. S. Army Missile Command

Contract No. DAAH01-74-C-0229

School of Electrical Engineering
Georgia Institute of Technology
Atlanta, Georgia 30332

QUARTERLY PROGRESS LETTER

on

INVESTIGATION OF FIELD EMISSION ELECTRON GUNS FOR GAS LASERS

Contract No. DAAH01-74-C-0229

This is the second Quarterly Progress Letter which covers the period from 12 January to 11 April 1974.

Pulsed emission measurements on a UO_2-W composite were made during this report period. These tests were performed in an existing glass/metal tube while awaiting delivery of specially designed high voltage experimental tubes. At the present time, the new 1.25 inch diameter, 20 inch long tube has been received, but the 4.5 inch size has not. The manufacturer states that delivery should occur within 10 days.

Before attempting electrical measurements, the vacuum system was processed by first baking the entire system in an oven to approximately 200 ^{o}C. After cooling, an rf coil was placed around the test envelope and energized with the 450 kHz induction generator. The sample, cathode, and anode were heated to about 800 ^{o}C. The upper temperature limit was set by the copper braze material. Heat was maintained until the pressure dropped into the low 10^{-7} Torr range. Operating pressure was in the 10^{-9} Torr range.

Initial electrical tests were performed using all ten stages of the Marx generator charged to approximately 18 kV/stage. Voltage waveforms were normal, but interelectrode breakdown was observed to occur. A faint blue glow was seen in the tube as was a "hot spot" located on the emitter edge along a crack. Breakdown was true interelectrode breakdown since the measurement circuit was guarded against surface leakage. Successive shots produced no change in the location of the hot spot.

Stages were progressively removed from the generator until no evidence of breakdown was observed. Only occasional breakdown was seen with six stages, and

none was observed with four stages. A reproduction of typical experimental data is shown in Figure 1. Since the area of the emitter was about 0.3 cm^2, current densities of 10 mA/cm^2 were obtained.

Calculations made using a crude model for the electron emitter connected in the appropriate equivalent circuit, yielded qualitative argeement with measured time-current behavior. No attempt was made to optimize the emission model for the particular sample used in the tests.

A new sample has been prepared for testing at, hopefully, the maximum Marx voltage. The new sample has rounded edges which should reduce the potential gradients and attendant acring. This sample is installed in the same glass envelope as used previously. The new larger envelope is being fitted with a special mount which will accept a variety of cylindrical samples. The rounded surfaces of the mount make it unnecessary to undertake tedious grinding of the composites. A second ion pump will also be used to allow testing of two samples simultaneously.

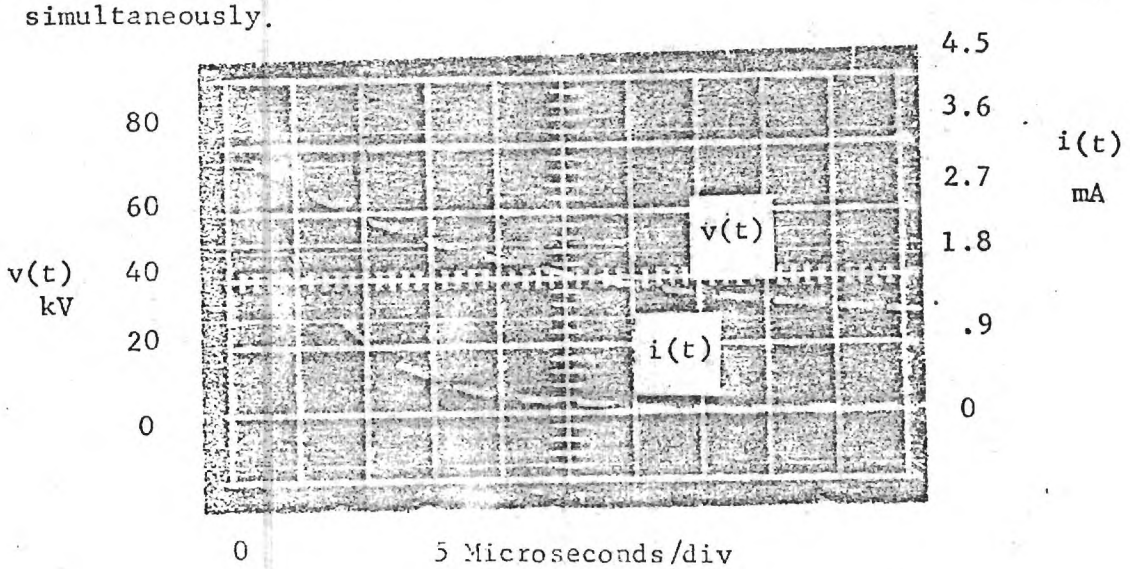

Figure 1. Typical Pulsed Emission Data.

QUARTERLY PROGRESS LETTER

12 April - 11 August 1974

INVESTIGATION OF FIELD EMISSION ELECTRON GUNS FOR GAS LASERS

U. S. Army Missile Command

Contract No. DAAH01-74-C-0229

School of Electrical Engineering
Georgia Institute of Technology
Atlanta, Georgia 30332

QUARTERLY PROGRESS LETTER

on

INVESTIGATION OF FIELD EMISSION ELECTRON GUNS FOR GAS LASERS

Contract No. DAAH01-74-C-0229

This is the third Quarterly Progress Letter, which covers the period from 12 April to 11 August 1974.

In order to eleminate previously observed breakdown along the inner surface of the glass vacuum envelope, a new tube having a 20 inch leakage path was fabricated and installed on the vacuum system. The same sample as tested previously in the short tube was used with a fixed electrode spacing of about 3 cm. Both electrodes were machined with rounded and polished edges to minimize potential gradients. After initial bakeout, the operating pressure stabilized at about 4×10^{-9} Torr. The system was first operated in the dc mode, but due to the large interelectrode spacing, a maximum current of 2×10^{-11} A could be realized with 50 kV applied. The circuit was reconnected for pulsed operation and the Marx generator used to apply approximately 100 kV to the diode giving an apparent current of 10 mA maximum. Several shots yielded consistient results. The series resistor of approximately 200 k ohms was shorted and the Marx generator triggered. With the series resistor removed, a breakdown, apparently from the anode to the glass tube, was observed.

After these tests, the diode was disassembled and modified so that a linear motion feedthrough could be used to vary the interelectrode spacing. Range of movement was approximately 2.5 cm. The same emitter was reinstalled in the modified diode. After bakeout, extensive dc date were taken. A series of V-I curves were obtained with the interelectrode spacing as a parameter. Such data are valuable in extrapolating emitter performance to

other voltage and spacing regimes. A maximum current of approximately 0.7 mA at 49 kV and 0.225 inch spacing was obtained. The use of smaller spacings at the maximum voltage (50 kV) resulted in vacuum breakdown. Pulsed testing was started upon completion of the dc measurements. Only two Marx stages were used in the first pulsed tests to provide duplication of the dc potentials used. These experiments showed an apparent maximum pulsed current of about 7mA at 40 kV, an order of magnitude larger than the observed dc emission. It was soon noted that when the electrode spacing was varied, the apparent emission current remained constant. Obviously, the largest contribution to the observed current was not field emission. It was hypothesized that the observed current was a combination of emission current and capacitive charging current. The following equivalent circuit was proposed.

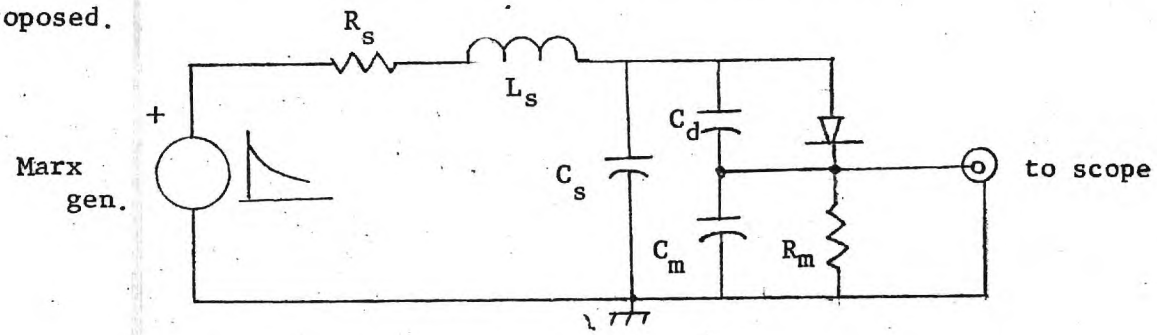

Here, L_s and R_s is the lead inductance and resistance, C_s is the anode-ground stray capacitance, C_d is the diode interelectrode capacitance, while C_m and R_m are associated with the measurement circuit. A direct measurement of C_s in parallel with the combination of C_d and C_m yielded a value of 15.5 pF. Further measurements showed that C_d was changed only slightly with diode interelectrode spacing, and was determined largely by the anode/cathode support structures.

Analog and digital simulation of a linearized version of the above circuit agreed well with the observed experimental behavior provided that L_s and R_s were chosen so that the system was heavily damped. With this

theoretical insight, R_s was increased to 3 megohms so as to greatly decrease the transient current. With this accomplished, emission current unambiguously observed. A current of about 1 mA, consistient with dc data, was obtained at 50kV.

A new sample was available at this time, so the diode was dissembled for installation in a recently completed 2.5 inch diameter glass vacuum envelope. The variable spacing feature was retained when the new sample was installed in the large envelope.

Direct current tests with the new sample (AMC-3) produced considerbly higher current at the same voltage and spacing than did the previous emitter. This behavior was expected since AMC-3 had sharp pins as opposed to the blunt pins used earlier. Direct current measurements gave about 4mA ($12mA/cm^2$) at 44kV.

When pulsed measurements were ready to be made on AMC-3, AMC was contacted in hopes of obtaining a transient voltage monitor and technical assistance with related instrumentation problems. The voltage monitor was needed to supplement the available indirect indication of diode voltage. A capacitive voltage divider provided by AMC was connected into the circuit in parallel with the experimental diode. Since additional transient current had to be supplied to the divider, the series water resistance was reduced to approximately 100 k ohms by the addition of $CuSO_4$ solution. Using six Marx stages, total currents of 12-15 mA were obtained with a spacing of 0.170 inch and an anode voltage of 50kV. These values were in reasonable agreement with experimental dc data. Typical results are shown in Figure 1. Note that the onset and duration of the emission are sharply defined.

The available Marx voltage was increased by the addition of four additional stages (total 10) and pressurization of the spark gaps.

The interelectrode spacing was set at 0.380 inch and data were taken as a function of anode potential. At this spacing a maximum current of about 13 mA was obtained at a voltage of 90kV. Attempts to obtain larger currents resulted in breakdown of the diode, usually at the edge of the emitter. Upon determination of the limitation at the 0.380 inch spacing, the diode was opened to maximum spacing of 0.462 inch. At this spacing, 105 kV could be used before breakdown occurred. The maximum current was again about 13mA. The capacitive component of the current was noticeably larger. Preliminary evidence indicated that the point of breakdown was shifting to slightly lower macroscopic electric fields (V/d) as the diode spacing was increased. It was also believed that edge effects at the anode and cathode were contributing to the observed breakdown. Therefore, the tube was disassembled and a larger diameter anode fabricated.

After reinstallation and pumpdown, the diode was opened to larger spacings in an attempt to operate at higher voltages. Operation was successful at a maximum of about 120 kV, but with no increase in emission. Capacitive current continued to increase and presented a problem when extracting the emission component of the total current. (This problem may require the use of null-balance techniques when operating near 200kV.) Since breakdown was still a problem, it was decided to remove the sample, repolish, reetch and remount it with the emitter flush with the sample holder.

Sample AMC-3 was reprocessed and replaced in the test facility. After bakeout, dc emission testing was initiated. At the minimum interelectrode spacing of 0.28 inch, a current of 360 μA was obtained at 50kV. While this test was in progress, the dc high voltage power supply failed, temporarily terminating the experiment.

It is planned to continue with dc and pulsed testing of this and larger samples. It is believed that improved mounting techniques will allow higher voltages and currents without breakdown.

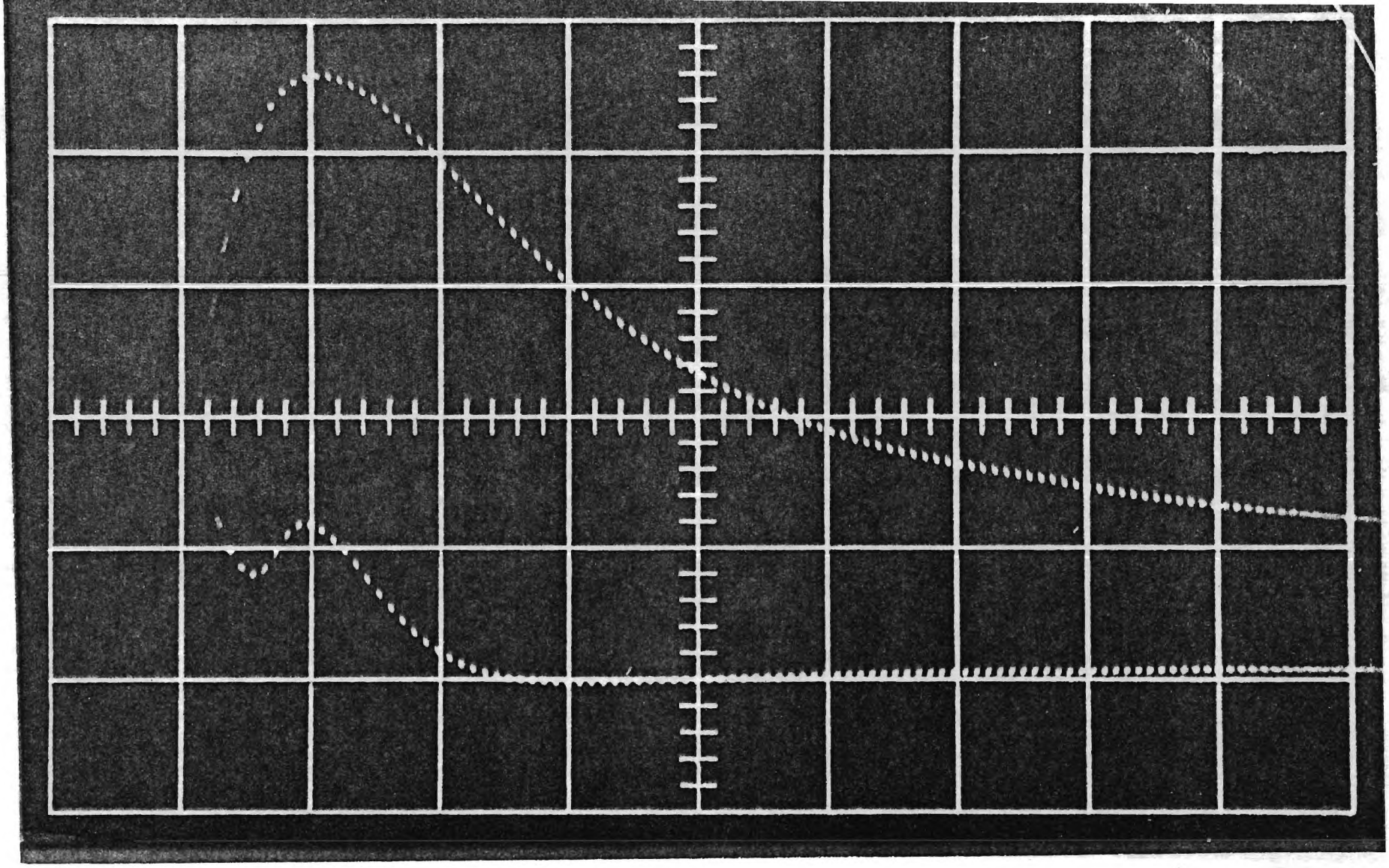

Figure 1. Field Emission Diode Current and Voltage as a Function of Time. Upper trace; 10 kV/div; Lower trace, 10 mA/div; Time scale, 10 μs/div; zero offset 1 div up and 1 div right.

E-18-6006
E-21-6

QUARTERLY PROGRESS LETTER

12 August 1974 to 11 January 1975

INVESTIGATION OF FIELD EMISSION ELECTRON GUNS FOR GAS LASERS

U. S. Army Missile Command

Contract No. DAAH01-74-C-0229

School of Electrical Engineering
Georgia Institute of Technology
Atlanta, Georgia 30332

QUARTERLY PROGRESS LETTER

on

INVESTIGATION OF FIELD EMISSION ELECTRON GUNS FOR GAS LASERS

Contract No. DAAH01-74-C-0229

This is the fourth Quarterly Progress Letter, which covers the period from 12 August 1974 to 11 January 1975.

As previously reported, sample AMC-3 was reprocessed and replaced in the test apparatus with the emitter surface flush with the sample holder. Dc emission testing had been initiated at the time the high voltage dc power supply failed. After some delay in obtaining the required parts, repairs were effected and testing continued.

A dc current of 305 μA was observed at 45 kV and 0.280 inch spacing. Pulsed emission testing resulted in diode breakdown with no observed emission current. Reinstalling the sample so that the emitter surface was approximately 0.050" above the holder surface produced a significant improvement in dc emission, approximately 1.5 mA being obtained at 30 kV and comparable interelectrode spacing.

Pulsed emission testing with this sample geometry was again characterized by arcing with no emission current observable at applied fields below that necessary for arc initiation.

Following this, a series of experiments to demonstrate the emitter area-emission current scalability were initiated. A sample holder capable of holding up to three 1/4" diameter samples (0.3 cm^2 area per sample) was mounted in the diode, and the first test was run using a single sample, AMC-4. The pins were pointed and 10-12 μm in length; the sample was mounted

protuding approximately 0.003 inch above the holder, as this geometry was expected to give the best results based on previous experience. Dc testing at a gap of 0.125 inch gave a maximum current of 400 μA at 16.0 kV.

Pulse testing commenced following the dc testing using an applied voltage of about 24 kV. The interelectrode gap of the diode was steadily decreased until emission current was evident. Figure 1 shows the maximum emission current of 303.5 mA obtained at a spacing of 0.138 inch. (Macroscopic field = 7.2×10^4 v/cm.) Higher voltages or closer spacings produced arcing. Before further tests were performed in the pulse mode, a nulling capacitor previously devised to cancel the diode capacitive current was reinstalled and adjusted to remove the initial current spike evident in Figure 1. Using this technique a nearly perfect zero line was obtained in the absence of emission current.

With the nulling capacitor, results such as that shown in Figure 2 were obtained. In this instance both voltage and current traces are displayed and several interesting features should be noted. First a current of approximately 2 mA was obtained at a spacing of 0.128 inch and an applied voltage of 23 kV providing a standard set of conditions for scalability testing as additional samples are added. Also, the non-linearity of field emission current with voltage is very clearly shown and the beneficial effect of the nulling capacitor is clearly demonstrated.

Upon completion of this test sequence, the diode was disassembled and a second sample, AMC-5, was put in place, thereby doubling the emitter area. The second sample was mounted in as nearly identical a fashion as possible to the first sample, protruding approximately 0.003 inch above the sample holder surface. Pin geometry was similar with fiber lengths of about 12 μm. Dc testing was continued for a substantially longer period of time than in previous tests. This conditioning appeared to be beneficial, as a maximum

current of 3.7 mA was obtained at 13.0 kV and 0.125 inch nominal spacing. This current may be somewhat misleading since later measurements showed that a spacing decrease of up to 0.030 inch could be expected from anode and anode support rad heating at the 50 W power input to the anode.

Pulse testing was commenced immediately upon dc test shut down in order to take advantage of any conditioning and cleaning that might have occurred. Initial results at an applied voltage of 15 kV and an inter-electrode spacing of 0.060 inch are shown in Figure 3. (Macroscopic field = 9.9×10^4 v/cm.) A peak current of 11 mA was obtained with no arcing at this substantially higher macroscopic electric field value.

Twenty-four hours later, with the system cold, results as shown in Figure 4 were obtained at an applied voltage of 19.0 kV and a spacing of 0.102 inch, or a macroscopic electric field value of 7.35×10^4 v/cm. A peak current of 7 mA was obtained prior to arc imitation. It would appear that cleaning and conditioning by dc operation have a beneficial effect on emitter performance.

To show scalability of emitter performance the previously established test conditions of 23 kV applied voltage and 0.128 inch spacing were used in obtaining the results shown in Figure 5. The 4 mA current under these conditions is double that shown in Figure 2, and given a preliminary indication of linear current scalability.

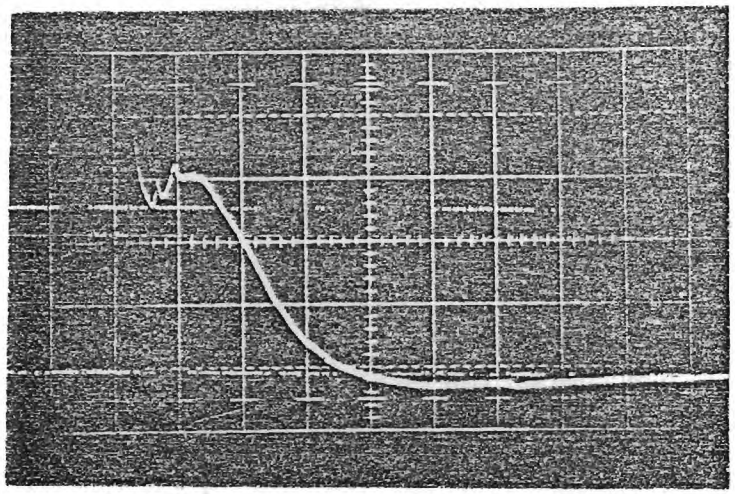

Figure 1. Maximum emission current obtained in pulsed operation with single 0.3 cm^2 area sample. Applied voltage 24 kV, inter-electrode spacing 0.138 inch. Vertical = 1 mA/div, horizontal = 20 microseconds /div.

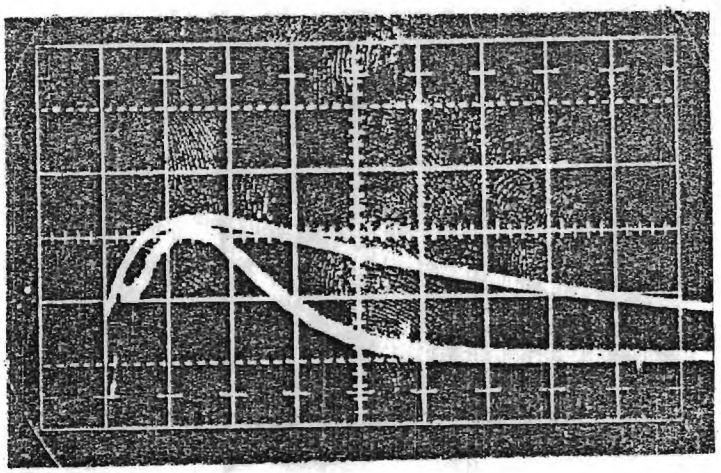

Figure 2. Current obtained from single 0,3 cm^2 area sample under conditions for scalability testing (lower trace). Upper trace is applied voltage. Current scale = 1 mA/div, voltage scale = 10 kV/div. Horizontal scale = 20 microseconds/div.

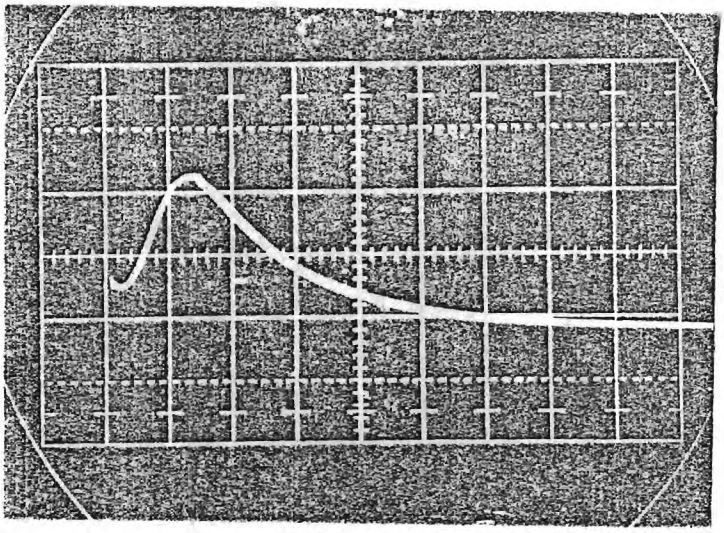

Figure 3. Maximum current obtained in pulsed operation with two samples each one of 0.3 cm^2 area. Applied voltage 15 kV, interelectrode spacing 0.060 inch. Vertical = 5 mA/div, horizontal = 20 microseconds/div.

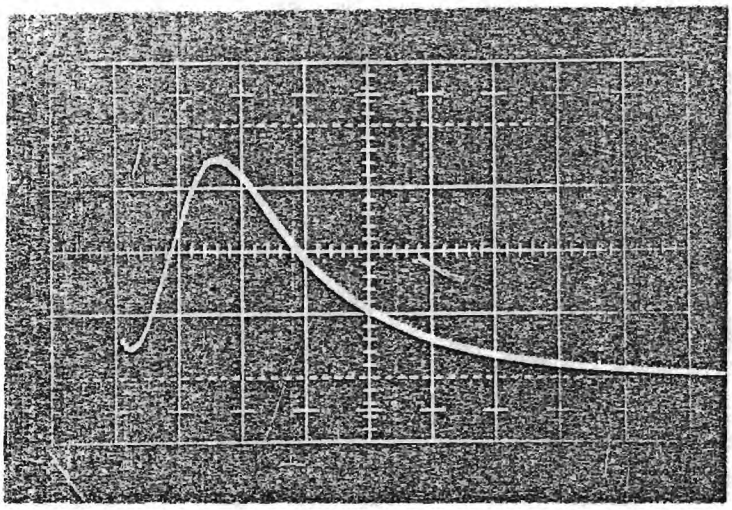

Figure 4. Maximum obtainable pulse emission current from two samples with system cold. Applied voltage 19 kV, interelectrode spacing 0.102 inch. Vertical = 2 mA/div, horizontal = 20 microseconds/div.

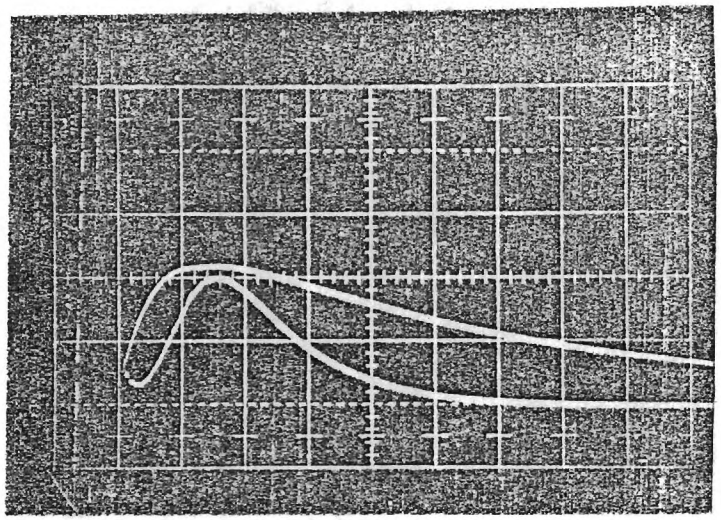

Figure 5. Total current obtained from two 0.3 cm^2 area samples under scalability testing conditions (lower trace). Upper trace is applied voltage. Current sensitivity = 2 mA/div, vollage sensitivity = 10 kV/div. Horizontal = 20 microseconds/div.

E-18-606
E-21-636

QUARTERLY PROGRESS LETTER

12 January 1975 - 11 May 1975

INVESTIGATION OF FIELD EMISSION ELECTRON GUNS FOR GAS LASERS

U. S. Army Missile Command

Contract No. DAAH01-74-C-0229

School of Electrical Engineering
Georgia Institute of Technology
Atlanta, Georgia 30332

QUARTERLY PROGRESS LETTER

on

INVESTIGATION OF FIELD EMISSION ELECTRON GUNS FOR GAS LASERS

Contract No. DAAH01-74-C-0229

This is the fifth Quarterly Progress Letter, which covers the period from 12 January 1975 to 11 May 1975.

During this report period the scalability tests discussed in the last report were completed. A third sample was added to the diode giving a total area of approximately 0.9 cm^2, and pulse testing was accomplished under the conditions of the tests performed with one and two samples.

An emission current of 6 mA was obtained under the conditions previously used with one and two samples of 0.125" spacing and 23 kV applied voltage. This result supports the assumed linear relationship between emission current and emitter area since currents of 2 mA and 4 mA were obtained with areas of 0.3 cm^2 and 0.6 cm^2 (one and two samples, respectively) as previously reported.

An attempt to achieve the maximum current from this emitter area was precluded by destructive arcing of the sample during a DC conditioning operation.

The low current densities achieved by the samples used for the scalability test series are accounted for by the extremely high fiber densities of these three samples. They are all in the range of $22 - 27 \times 10^6$ fibers per cm^2. It was known at the time that these samples were far from optimum, but their use allowed demonstration of scalability at a time when better samples of lower density were unavailable.

Subsequent to the completion of the scalability test series a low density sample of approximately 6×10^6 fibers per cm^2 was prepared for testing. In conjunction with this sample an anode of arc-fused molybdenum was installed in place of the stainless steel or porous, sintered molybdenum materials used previously.

DC operation of this sample prior to pulsing gave approximately 9 mA emission current at 0.035" spacing and 7 to 8 kV applied voltage. This is substantially better than routine values of previous experiments. Pulse testing of the sample commenced after 160 hours of DC operation and reduction of pressure, with the anode hot, to 2×10^{-8} torr. A cold system pressure of 3×10^{-9} was observed. An emission current of 18 mA (current density of 60 mA/cm^2) was observed at an applied macroscopic field of 8.4×10^4 V/cm. This breakdown threshold field is somewhat higher than previously observed in a cold system; and it is felt that the combination of lower emitter tip density, less porous anode, and more comprehensive conditioning and anode outgassing are the primary factors influencing the improved results.

This same sample was re-etched with longer fibers (approximately 15 μm versus 10 μm in the previously described test) and remounted in the diode for testing. Very poor DC emission performance was observed and the sample was removed without pulse testing. It is felt that the poor performance of this sample is related to emitter mounting geometry and is in no way related to the increased pin length.

After re-etching to obtain 10 μm fibers as previously used the same sample was once again mounted in the diode for testing. Particular attention was paid to the position of the sample in the sample holder, and the

pin tips were placed approximately 80 μm above the plane of the sample holder surface. DC operation was continued for nearly 500 hours, with 2.0 mA emission current obtained after 150 hours; and 2.0 to 2.5 mA current being maintained for the remaining 350 hours. At the end of this period the pressure with the anode hot was approximately 7×10^{-9} torr and a cold system pressure of 2×10^{-9} torr was achieved. After extensive pulse testing a gross emission current of 38 mA was obtained (current density 125 mA/cm^2) at an interelectrode spacing of 0.285" and an applied voltage of 106 kV. This is a macroscopic field of 1.5×10^5 V/cm or another incremental increase in breakdown threshold field. It is felt, in addition to the factors previously cited, that the sample holder-emitter geometry has a significant effect on the breakdown field through minimization of field concentration at the sample edges.

Work is continuing to extend the voltage region to the 150 - 200 kV range, and to define the factors limiting the operating field strength.

E-18-606

DAAH01-74-C-0229

INVESTIGATION OF FIELD EMISSION ELECTRON GUNS FOR GAS LASERS

By:

R.K. Feeney
W.L. Ohlinger
A.T. Chapman
J.K. Cochran

Final Report for Period 12 October 1973 – 31 August 1975

Approved for Public Release; Distribution Unlimited

Prepared for:

High Energy Laser Systems Project Office
U.S. Army Missile Command
Redstone Arsenal, Alabama 35809

Army High Energy Laser Directorate
U.S. Army Missile Command
Redstone Arsenal, Alabama 35809

1976

1 April 1976

Georgia Institute of Technology
Schools of Ceramic and Electrical Engineering
Atlanta, Georgia 30332

DAAH01-74-C-0229

INVESTIGATION OF FIELD EMISSION ELECTRON GUNS FOR GAS LASERS

By:
R. K. Feeney
W. L. Ohlinger
A. T. Chapman
J. K. Cochran

Georgia Institute of Technology
Schools of Ceramic and Electrical Engineering
Atlanta, Georgia 30332

1 April 1976

Final Report for Period 12 October 1973 - 31 August 1975

Prepared for:

High Energy Laser Systems Project Office
U.S. Army Missile Command
Redstone Arsenal, Alabama 35809

Army High Energy Laser Directorate
U.S. Army Missile Command
Redstone Arsenal, Alabama 35809

TABLE OF CONTENTS

LIST OF FIGURES

LIST OF FIGURES (Cont'd)

Foreword

The Schools of Ceramic and Electrical Engineering of the Georgia Institute of Technology, Atlanta, Georgia prepared this report on an Investigation of Field Emission Electron Guns for Gas Lasers under Contract No. DAAH01-74-C-0229.

The program was sponsored by the Army High Energy Laser Systems Project Office and the program monitor was Mr. Charles Cason, Army High Energy Laser Directorate, U.S. Army Missile Research, Development and Engineering Laboratory, U.S. Army Missile Command, Redstone Arsenal, Alabama. Dr. R. K. Feeney was the Project Director.

Principal co-authors of this report were R. K. Feeney, W. L. Ohlinger, A. T. Chapman, and J. K. Cochran.

Publication of this report does not constitute U.S. Army approval of the report's findings and conclusions. It is published only for the exchange and stimulation of ideas.

SECTION I

Introduction

The evolving technology of melt-grown oxide-metal composites has developed to a state such that these materials may now be grown of sufficient size to be considered for many useful applications. The materials are considered here as a candidate for electron beam gun cathodes, as well as high-voltage current disconnects. Both heated thermionic and thin foil cold cathodes have found use in large area electron beam gas lasers. The oxide-metal composite materials which are rugged structures having precisely repeatable electrical characteristics were assessed as a promising replacement for the delicate, conventional emitters. This report presents pertinent tests and evaluations of these materials for the e-beam gun application. The most important points considered by the effort were the scaling of existing voltage levels of 2 kV to the 150 kV range required by the lasers, and the verification that, at these voltage levels, the emitter size could be scaled to provide the necessary beam current. The present program was directed toward pulsed mode operation at a voltage of 150 kV while providing an emitted current density of 100 mA/cm^2 of emitter material. Total current scaling over the range of 0.3 cm^2 to 3 cm^2 of emitter area was also an objective.

The degrees to which these criteria were met are outlined in Sections III and IV of this report. These discussions are preceded by a description of the experimental apparatus and experimental

procedures. A fabrication cost estimate which facilitates comparison with other emitter types is included. A mechanism responsible for the failure of the emitters and design precautions are discussed. A final chapter gives conclusions and recommendations.

Before presenting these results, it is appropritate to provide a description of the materials and their fabrication process. The material is included for completeness and additional details may be found elsewhere.[1]

The composites, consisting of an oxide matrix containing millions of less than 1-μm-diameter metal fibers per cm^2, were grown from near eutectic compositions using a direct rf-heating internal floating-zone technique. This technique eliminates the usual containment and contamination problems, since the molten zone is self-contained by its unmelted outer surface or skin. Very uniform composites are produced because of the well-defined liquid-solid interface associated with the inherent steep temperature gradients.

The samples, from which emitter structures were formed, were fabricated by first dry mixing the desired proportions of high-purity oxide and metal powders. This mixture was pressed into a cylindrical rod 19 mm in diameter by about 38 mm in length, and sintered inside an inductively heated Mo preheat tube using rf heating at 3.5 MHz. A dynamic atmosphere of N_2 and/or CO/CO_2 flowed through the quartz containment tube to provide the neutral or reducing environment necessary to prevent the oxidation of the metal powder in the rod and the Mo preheat tube. Preheat temperatures of 1500°C were required to sinter the sample rods and to increase their electrical conductivity

sufficiently for direct rf heating when the Mo preheater tube was lowered out of the rf field. Direct heating further increased the temperature until the interior of the rod melted. The high radiant heat loss from the surface of the rod and the relatively low thermal conductivity of the oxide-metal mixture produced a steep thermal gradient across the skin of the rod and maintained a surface temperature well below the melting point of the oxide-metal eutectic.

Unidirectional solidification was achieved by moving the molten zone upward through the rod at 2-4 cm/hr. A cavity formed over the molten zone because of the difference in density between the porous sintered rod and the nearly void-free solidified composite.

During the lowering of the rod, the oxide-metal mixture melted from the roof of the cavity, ran down the interior walls of the pellet into the molten pool, and was unidirectionally solidified at the base of the molten zone. To prevent thermal cracking, the rod was lowered into the Mo preheat tube which was repositioned in the lower turns of the induction coil to act as a postheater operating at 1500°C. After the rod was lowered several cm, the Mo tube was raised to heat the entire length of the rod and control its rate of cooling.

Suitable selection of growth conditions formed structures containing between 5×10^6 and 50×10^6 fibers/cm^2 with fiber diameters between 0.2 and 1.0 μm. Chemical etching was used to expose and shape the arrays of tungsten pins. Examples of the variety of possible pin-shapes will be discussed in later chapters of this report.

SECTION II

Experimental Apparatus and Procedures

The equipment and procedures used in the emission test program were designed to facilitate valid comparisons between various emitter samples. The main emphasis of the work performed was the achievement of maximum current densities, highest possible working voltages, and the determination of the most desirable cathode and anode geometries. In this section general descriptions of the samples, experimental apparatus, and experimental procedures are presented.

A. Emitter Preparation

All samples used in this work were composites composed of 0.3 to 0.9 μm diameter tungsten fibers arrayed in a matrix of uranium dioxide. Typical fiber densities ranged from 5.75×10^6 to nearly 30×10^6 pins/cm^2. All samples were made in a similar fashion.

Slices of material 0.5 to 1.5 mm thick were cut from the cylindrical pellets used for the internal molten zone growth process by which the composites were created. After polishing microscopic inspection allowed assessment of the fiber growth uniformity and selection of a suitable slice of material for use as an emission sample. To facilitate mounting in the emission testing apparatus, the composites were brazed with copper to 1/4" diameter molybdenum support pins. These support pins were of such a geometry that they were also compatible with the mounting stage of a scanning electron microscope which was used to assess pre- and post-emission pin geometries. After brazing, the samples

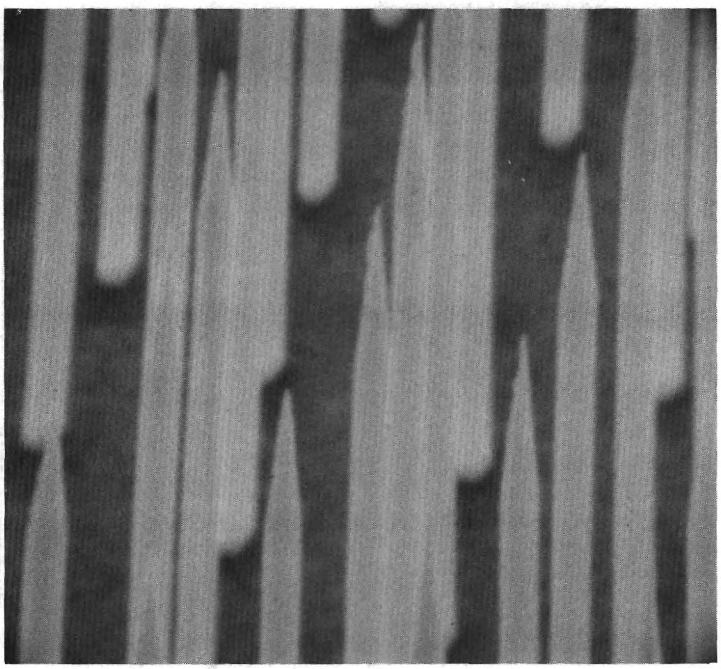

Figure 1. Scanning Electron Micrograph of Typical Emitter-Pin Geometry, X12300.

were chemically etched using previously developed etchant compositions and procedures to produce either blunt or conically-pointed fibers of 10 to 15 μm height.[2] Typical fiber geometries are shown in Fig. 1.

B. Experimental Apparatus

The experimental apparatus was designed to provide a vacuum environment of 10^{-8} Torr while allowing the test emitters to be operated at up to 200 kV. The capability of vacuum processing of the experimental tube structure by induction heating was also provided.

1. Experimental Tubes and Vacuum System

The final experimental tube design consisted of a length of pyrex glass tube with glass tube-to-Conflat-flange transitions on each end. Tubes of 1.5 and 2.5 inches o.d. were used, with most of the work being accomplished with the larger tube. Flash-over requirements were met up to 200 kV with a glass tube length of about 20 inches. The tube was attached at its lower end to one branch of a stainless steel cross; the remaining three branches of which led to a Veeco Mag Ion (Model MI-150) pump of 150 1/s capacity, a roughing pump (sorption type or trapped mechanical type), and an electrical signal current feedthrough. The ion pump was baked by internal heaters, while the vacuum plumbing and experimental tube were baked with electric heating tapes. The normal bakeout temperature was about 100°C which provided a static system pressure of about 3×10^{-9} Torr. A coupling coil made from 1/4 inch copper tubing was positioned around each experimental tube. This coil was used with a 7.5 kW, 450 kHz rf generator to provide a high temperature bakeout of the structures within the experimental tube.

The emitter support structure was mounted with small porcelain insulators to a plate between the experimental tube and the cross, thus isolating the emitter and the electrical feedthrough from the experimental tube. This arrangement prevented the inclusion of any leakage current in the measured current. At the upper end of the experiment tube was affixed a Varian linear motion feedthrough (Model 954-5049) allowing a 2.5 cm range of motion. The anode was attached to this feedthrough via a support rod. Provision was made for easily changing the anode so that various types of geometries could be used. The entire enclosure was constructed of glass or stainless steel, and internal components were of stainless steel or molybdenum. All seals were of the copper-gasketed Conflat type, and a gold-seal ultra-high vacuum valve was employed for isolation from the rough pumping system.

2. Power Supplies and Instrumentation

Dc Operation. Operation of the test diode under both dc and pulse conditions was employed in the experimental work. For dc operation power supplies of up to 50 kV and 5 mA (del Electronics 50TC-5-1) or 12 kV and 250 mA (Sorenson 2012-250) capacity were available. When operating under dc conditions, a current limiting resistor was utilized in series with the test diode. A Hewlett Packard 3430A Digital Voltmeter was used to determine the potential applied to the diode. Emission current was measured with a Keithley 610R Electrometer.

Pulsed Operation. Pulsed testing of the emitters was accomplished with the experimental apparatus shown in Fig. 2. A schematic diagram of the experiment is shown in Fig. 3.

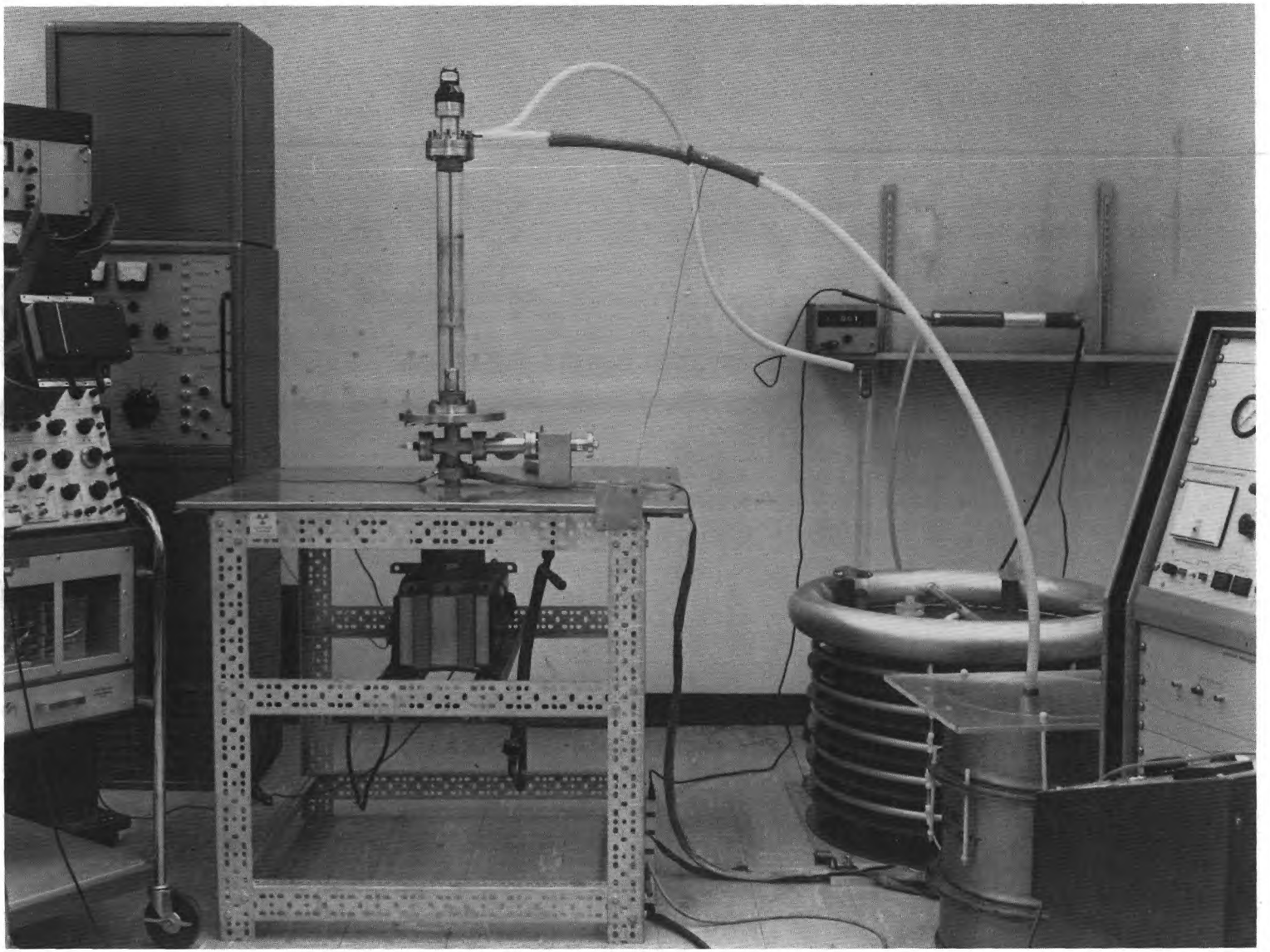

Figure 2. Overall View of Experimental Equipment Used for Pulse Testing of Field Emitters.

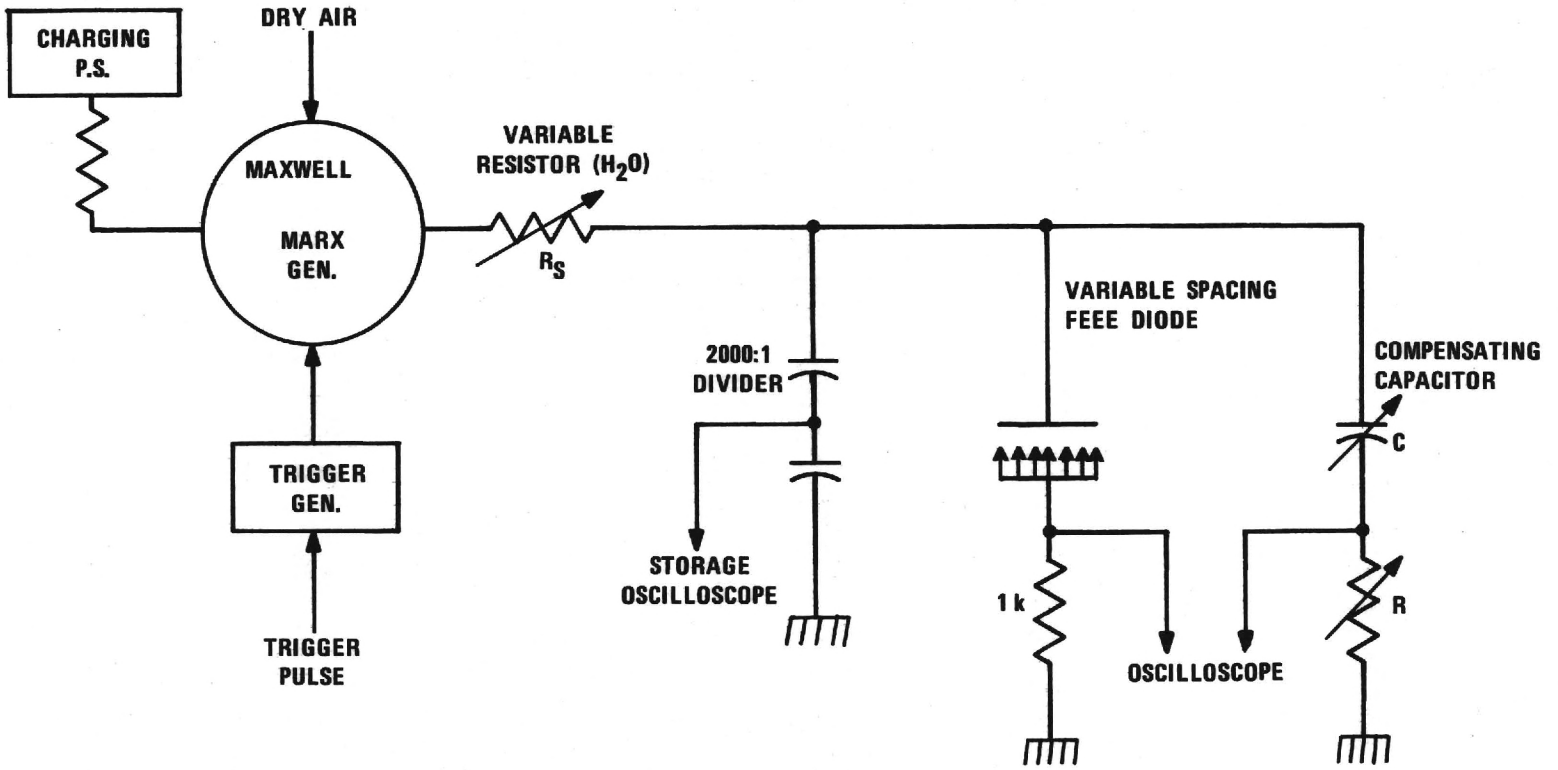

Figure 3. Schematic Diagram of the Experimental Apparatus.

The charging voltage and number of stages of the generator used could be adjusted to give a very wide range of output voltages. Measurement of the applied voltage was accomplished by use of a 2000:1 capacitive voltage divider whose output was displayed via a storage oscilloscope (Hewlett-Packard 141A) for reference purposes or photographed by an oscilloscope camera mounted on a Tektronix 545B oscilloscope for permanent recording. Current waveforms were permanently recorded by photographing the trace displayed on the Tektronix 545B oscilloscope.

A significant difficulty encountered in the pulsed emission current measurement was that introduced by the presence of capacitive transients. (See Fig. 4.) The anode-cathode capacitance of the FEEE diode was measured to be approximately 13.6 pF. The capacitance is determined primarily by the long support rods and the cathode, and consequently is relatively insensitive to spacing. This value of capacitance is sufficient to support a transient current many times the expected emission currents. The transient current can be reduced by increasing the size of R_s; however, this also reduces the magnitude of the voltage pulse, as well as delaying the occurrence of the voltage maximum. In order to make valid pulsed measurements, it was necessary to use a nulling technique to remove the capacitive transient current. This was accomplished by using an adjustable coaxial capacitor to sample the voltage pulse. The compensating signal, taken from the junction of R and C, was applied to one channel of a differential amplifier oscilloscope. The values of R and C were then adjusted to cancel, as nearly as possible, the capacitive transient

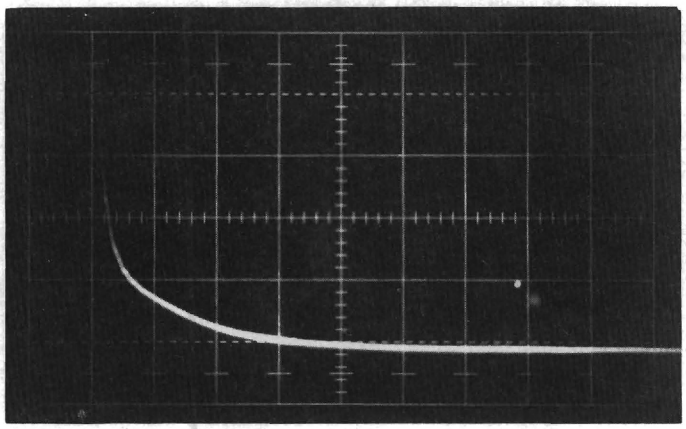

Figure 4. Typical Uncompensated Diode Current: Vertical, 2 mA/div; Horizontal, 10 μsec/div. Origin is 1 div up and 1 div right.

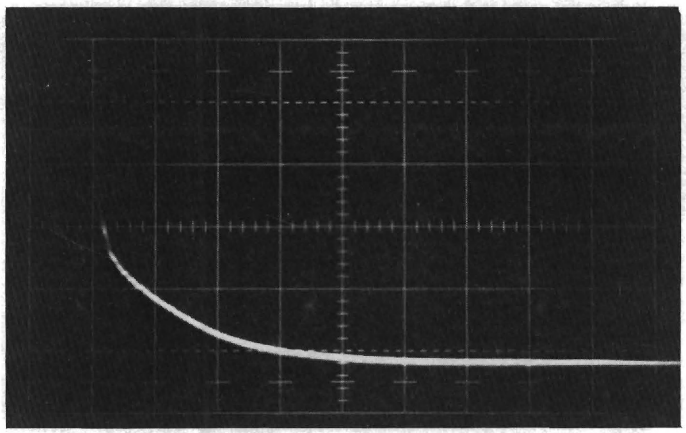

Figure 5. Typical Output Signal from Compensating Capacitor. Vertical, 1 mA/div; Horizontal, 10 μsec/div. Origin is 1 div up and 1 div right.

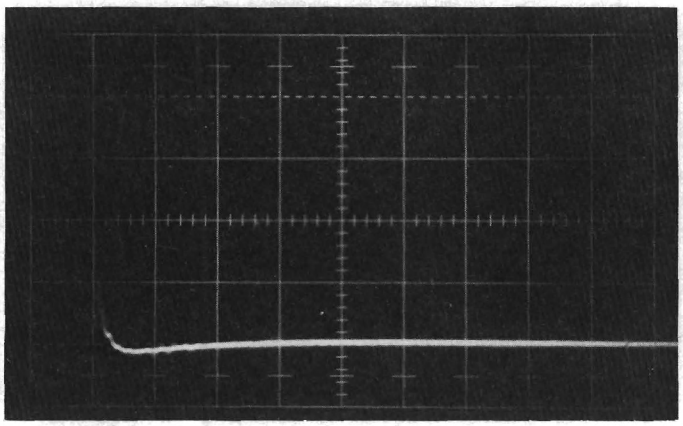

Figure 6. Typical Baseline Obtained by Subtraction of Signal Shown in Fig. 5 from that Shown in Fig. 4. Vertical, 2 mA/div; Horizontal, 10 μsec/div. Origin is 1 div up and 1 div right.

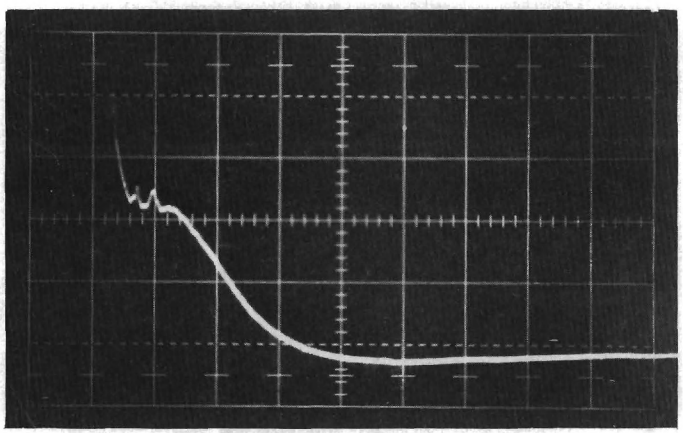

Figure 7. Typical Emission Current Waveform as Observed without Capacitive Current Compensation. Vertical, 1 mA/div; Horizontal, 20 μsec/div. Origin is 1 div up and 1 div right.

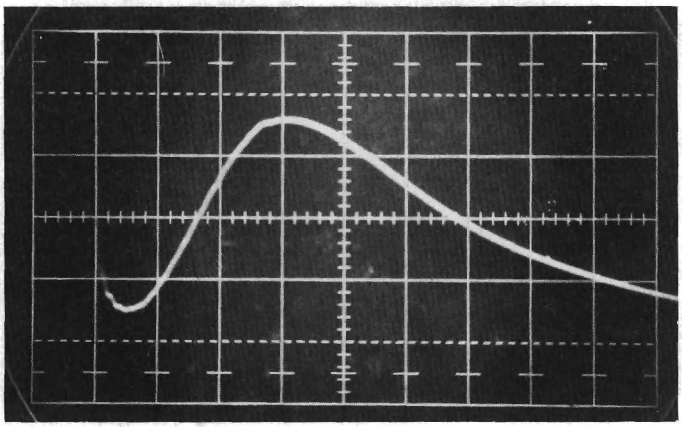

Figure 8. Typical Emission Current Waveform as Observed Using the Compensating Capacitor. Vertical, 2 mA/div; Horizontal 10 μsec/div. Origin is 1 div up and 1 div right.

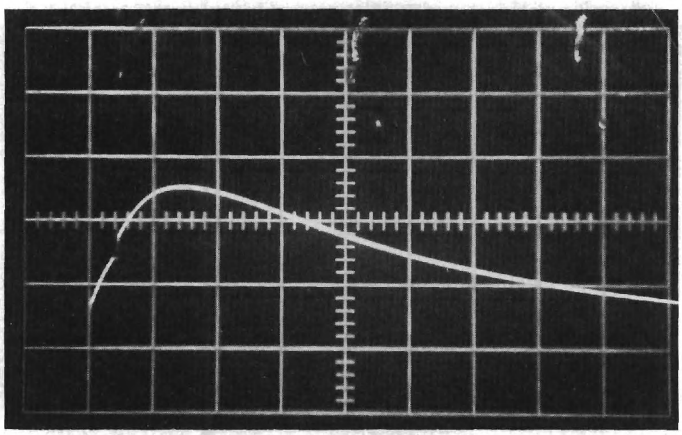

Figure 9. Typical Waveform of the Applied Voltage. Vertical, 10 kV/div; Horizontal, 20 μsec/div. Origin is 1 div up and 1 div right.

from the test diode. This adjustment was very critical because of the extremely high values of dV/dt at the high voltages. Since the anode-cathode capacitance was relatively independent of interelectrode spacing, minor changes in spacing could be made without readjusting the compensating capacitor.

Photos of various typical current waveforms are shown in Figs. 4-8. Included are: the uncompensated capacitive diode current (no emission current), Fig. 4; the compensating capacitor output current, Fig. 5; the base line obtained by adding the waveform of Fig. 4 and the inverted waveform of Fig. 5, Fig. 6; the emission current observed without capacitive current compensation, Fig. 7; and a typical emission current trace as observed using the nulling capacitor, Fig. 8. Figure 9 shows a typical voltage trace.

C. Experimental Procedures

Although the procedural details of the experiments were subject to considerable variation, several major routines were essentially standardized and are described in the following section.

Before installation in the test diode, the pin height and pin geometry of a sample were observed with an optical microscope and/or a scanning electron microscope. Photomicrographs allowed determination of factors of interest concerning the samples, such as pin density, pin height, and pin tip shape.

Following installation of the sample in the test diode, the vacuum system was rough-pumped using either a liquid nitrogen cooled zeolite sorption pump or a mechanical vacuum pump with a dry-ice-acetone cold trap on the fore line. When a pressure of less than

10 mTorr was achieved, the ion pump bakeout heaters were activated, and the pump baked for a minimum of one hour. Upon completion of bakeout, the ion pump was allowed to cool, and was then activated when the system pressure was less than 5 mTorr. The roughing pump was isolated from the remainder of the system at this time through a Granville-Phillips gold-seal ultra-high vacuum valve. The glass envelope and stainless steel parts of the system were then wrapped with heating tapes and baked at approximately 150°F until the pressure was essentially stable, normally 48 to 72 hours. At this time a pressure of 1 to 5×10^{-8} Torr was normally attained.

At this time the emitter was activated by application of about 2-10 kV dc. Direct current operation continued at current densities of 3 to 30 mA/cm^2 until the system pressure was stable at the maximum current density attained with the particular sample. During this period, system pressures greater than 1×10^{-6} Torr were prevented by limiting the emission current until reduced outgassing from the electron bombardment heated anode eliminated the possibility of such a pressure excursion. When increased current levels yielded no or only negligible pressure increases and the emission current showed minimal short range (in time, a few seconds) variations (usually less than ±1%), the dc conditioning operation was considered to be complete and pulse testing was commenced.

Pulse testing was normally initiated after the anode and anode support rod had cooled to room temperature and the interelectrode spacing was stable, i.e., not changing due to heating or cooling of the anode support. For initial testing, spacing was generally in the

range of 0.3 to 0.7 cm and applied potentials of 20 to 40 kV were commonly used.

Before the small emission currents could be unambiguously observed, it was necessary to adjust the nulling circuit. This was accomplished by operating the tube at a voltage below the threshold for emission and changing the values of C and R to produce a flat trace on the oscilloscope. Alternatively, since the interelectrode capacitance varied slowly with spacing, the spacing was increased sufficiently to preclude emission and the nulling time constant adjusted. This adjustment was very critical at the higher voltages.

Once a measurable pulse emission current was obtained (typically 1 mA) by increasing the voltage or decreasing the spacing gradually, an effort was then made to determine the maximum current obtainable without breakdown. Also, the maximum macroscopic applied field without encountering breakdown was recorded. In the series of experiments run to demonstrate current versus area scalability, an attempt was made to measure emission current under a fixed set of conditions reproduced as accurately as possible in each test. When it was felt that the maximum performance of a particular sample had been realized or the sample performance degraded due to breakdown damage, the sample was removed and inspected once again with the optical microscope and/or scanning electron microscope.

SECTION III

Experimental Results

This section discusses the experimentally observed electron emission performance of the materials. The objectives of these experiments were the experimental verification of emitter operation at voltages of at least 150 kV and the scalability of emission current with cathode area.

A chronological summary of the experimental results is given in Table I. The table summarizes the emitter parameters as well as presenting the principal results. These experimental results will be discussed in detail in the following chapters. The discussion is organized along topical lines.

A. Preliminary Experiments

The initial experiments utilizing samples numbered AMC-1 and AMC-2 produced a maximum of 1 mA emission current, and revealed several problem areas which were fairly well understood as a result of the five experiments (individual pumpdowns) run using these two samples. The problem of capacitive current masking the low level emission currents of these samples was encountered and investigated by operating the diode with no emitter installed. Several equipment changes, such as changing to the 2.5 inch diameter experimental tube and installation of the linear motion feedthrough allowing external adjustment of the interelectrode spacing, were made as a result of these initial experiments. The improved sample holder used with the

TABLE I

Summary of Pulsed Emission Experiments

Sample #	Tip Shape	Pin Height	Pin Density	Max Voltage	Max Macroscopic Fields	Max Pulse Current	Max Current Density	Remarks
AMC-1	Blunt	3-5μm	$10\times10^{6}/cm^{2}$	-	-	-	-	
AMC-2	Blunt	8-9μm	$16\times10^{6}/cm^{2}$	11kV(approx)	0.8×10^{5}V/cm	1mA	?	
AMC-3	Pointed	8-10μm	$24.7\times10^{6}/cm^{2}$	105kV	1.16×10^{5}V/cm	10mA approx.	$34mA/cm^{2}$	Sample mounted protruding approx. 0.003"-0.005" above sample holder surface, used capactive voltage divider for voltage measurement.
3a				120kV	1.02×10^{5}V/cm	10mA approx.	$34mA/cm^{2}$	Same sample as AMC-3, changed anode to 1-1/2" diam from 3/4" diam.
3/2	Pointed	11μm	$25\times10^{6}/cm^{2}$	90kV	0.77×10^{5}V/cm	None		Sample mounted flush with sample holder surface, used nulling circuit.
3/2a				90kV	0.52×10^{5}V/cm	None		Same sample as AMC-3/2, sample mounted protruding approx. 0.050" above sample holder.

TABLE I (Continued)

Sample #	Tip Shape	Pin Height	Pin Density	Max Voltage	Max Macro-scopic Fields	Max Pulse Current	Max Current Density	Remarks
3/2b				200kV(approx)	1.8×10^5V/cm	None		Same sample as 3/2 and 3/2a but used Al foil covered anode, sample mounted as 3/2a, no measurable current before anode foil destruction.
AMC-4	Pointed	10-12μm	$22.4\times10^6/cm^2$	24kV	0.76×10^5V/cm	3.5mA	$12mA/cm^2$	Sample mounted in three headed holder for scalability test, gave 2mA @ 0.125" spacing and 23kV.
AMC-5	Pointed	10-12μm	$24.2\times10^6/cm^2$	23kV	1.0×10^5V/cm	12mA	$20.4ma/cm^2$	Second scalability sample run with AMC-4 gave 4mA @ 0.125" spacing and 23 kV.
AMC-6	Pointed	11μm	$27\times10^6/cm^2$	23kV	0.73×10^5V/cm	6mA	$6.8mA/cm^2$	Third scalability sample, run with AMC-4 and 5 gave 6mA @ 0.125" spacing and 23kV.
AMC-7	Pointed	10-12μm	$7.5\times10^6/cm^2$	32kV	0.84×10^5V/cm	18mA	$61mA/cm^2$	Low fiber density sample, good performance.
AMC-8	Pointed	14-16μm	$6.2\times10^6/cm^2$	Not pulsed due to extremely poor dc performance				Rounded emitter surface and longer fibers, poor performance even with low density.

TABLE I (Continued)

Sample #	Tip Shape	Pin Height	Pin Density	Max Voltage	Max Macroscopic Fields	Max Pulse Current	Max Current Density	Remarks
AMC-9	Pointed	10μm	$5.76\times10^{6}/cm^{2}$	107kV	1.48×10^{5}V/cm	38mA	$130mA/cm^{2}$	Lower density, excellent performance.
9a 9b				Not pulsed due to anode failures				9a & 9b same sample as 9, but gridded anodes, no pulse data obtained due to anode failure
AMC-10	Pointed	10-12μm	$6\times10^{6}/cm^{2}$	46kV	2.13×10^{5}V/cm	None		Small diameter anode, 1/16" diam, no measurable pulse current obtained before breakdown.
AMC-11	Pointed	9μm	$4.6\times10^{6}/cm^{2}$	90kV	1.22×10^{5}V/cm	38mA	$130mA/cm^{2}$	Pin density reported is average value including "potholes." Density in growth areas is approx. $8\times10^{6}/cm^{2}$. Anode diam 3/4".

next sample, AMC-3, was also a result of information gathered in the course of the first experiments.

B. Voltage Scalability

The majority of the experiments were directed toward achieving the maximum emission current at the highest operating voltage. However, as current yield was increased, tendency for vacuum breakdown to occur also increased. Various anode and cathode configurations were tried to alleviate the breakdown problem while obtaining maximum emission current.

AMC-3 was the first sample to be mounted in the improved holding fixture, which incorporated a guard ring. The improved mounting geometry, coupled with a change in pin tip shape from blunt to sharp, resulted in significantly improved emission current. As can be seen in Table I, this sample was operated at voltages up to 105 kV and gave pulse currents of possibly as much as 10 mA. The current values for this sample could not be precisely determined since the nulling circuit used to cancel the capactive current was not added until the next experiment, which utilized this same sample. Experiment AMC-3a utilized a 1-1/2 inch diameter anode in place of the 3/4 inch diameter one previously used. No significant advantage of the larger anode was observed.

In experiments AMC-3/2 and AMC-3/2a the sample previously used in AMC-3 was tested, after re-etching, utilizing the compensating capacitor. In these two experiments, the sample was, respectively, mounted flush with the sample holder surface and protruding approximately 0.050 inch above it. As noted in the table, no pulse emission current was observed in either of these instances, and breakdown was

encountered at relatively low macroscopic field values.

Direct current operation of this sample produced a current of 305 mA at 45 kV and 0.280 in spacing when the emitter was flush with the cathode mount. Raising the emitter gave 1.5 mA at 30 kV. This test reinforced the importance of proper emitter mounting.

Examination of the anode used in the above dc test revealed a distinct ring-shaped mark. This ring was apparently the result of strongly preferred emission from the edge of the emitter.

An analysis of emitter mounting configurations, discussed later in the report, confirmed the tendency toward edge dominated emission. Another analysis performed at the same time indicated that reduced emitter pin density would provide increased emission when the diode was operated at the large spacing necessary for high-voltage operation.

To test the pin density hypothesis, sample AMC-7, having approximately 7.5×10^6 pins/cm^2, was prepared. This sample yielded the highest gross current and current density obtained to that time, and a slightly higher macroscopic field of 0.84×10^5 V/cm was achievable without breakdown. However, evidence still pointed to the conclusion that the majority of emission current was coming from the sample edge. A slightly convex emitter surface was therefore prepared as a solution.

Sample AMC-8 was prepared with the sample edge 25 μm lower than the center, and was mounted in the holder with the sample edges protruding 5 μm above the sample holder surface. Performance of the sample in dc operation was extremely poor and pulse testing was not attempted.

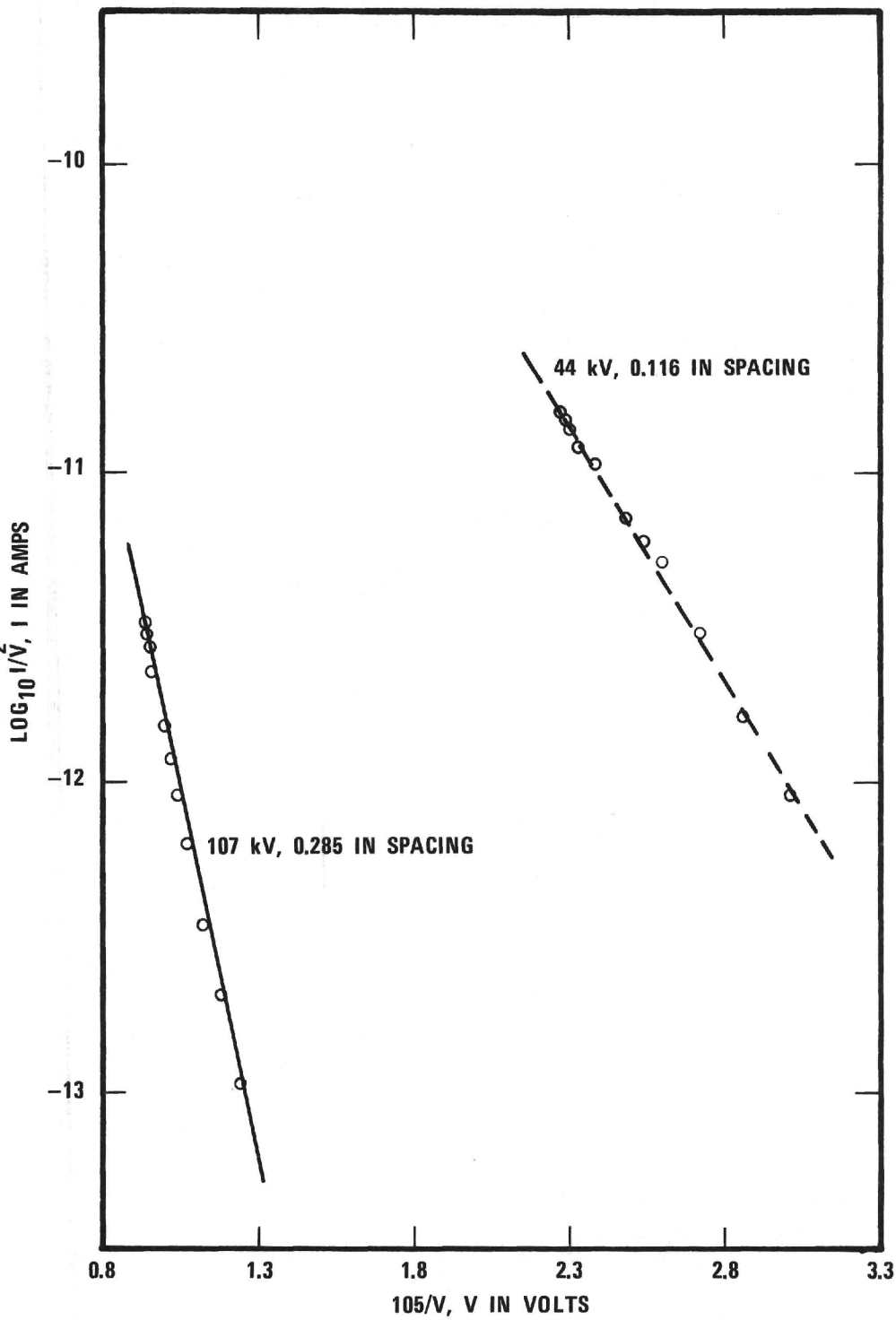

Figure 10. Fowler-Nordheim Curves Plotted from Current and Voltage Decay Traces for Two Operating Voltages, Sample AMC-9.

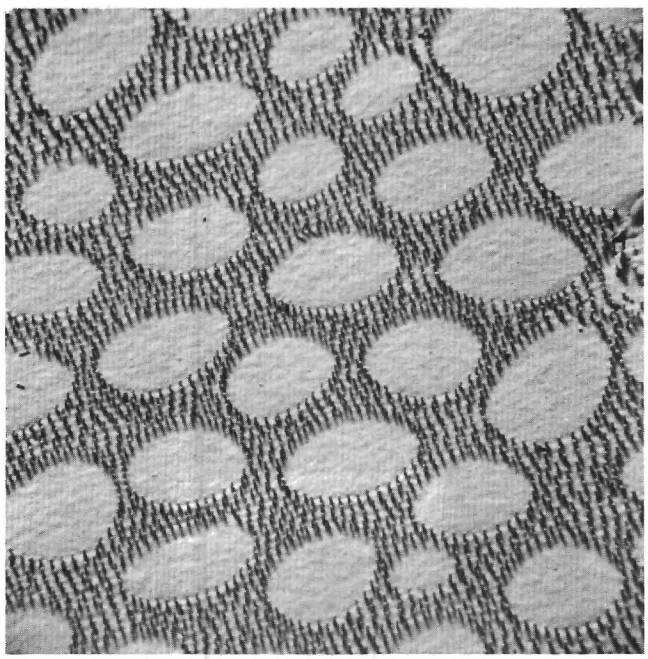

Figure 11. Photomicrograph of "Pot-Hole" Structure Utilized in Sample AMC-11, X500.

Upon removal of AMC-8 from the diode, the same sample was ground flat, repolished, and etched. Reinstalled in the diode as AMC-9, with the sample protruding approximately 80 μm above the sample holder, the best results of the project were obtained. Operating at up to 107 kV applied potential, a gross current of 38 mA was observed, indicating a current density of 130 mA/cm^2. Figure 10 displays two Fowler-Nordheim plots derived from the decaying portions of two different voltage-current traces obtained with sample AMC-9. One curve was obtained with a peak pulse voltage of 44 kV, and the other with 107 kV, representing a voltage increase factor of approximately 2.5. Calculation of the macroscopic field at the current cutoff point gives, respectively, 1.13×10^5 V/cm and 1.11×10^5 V/cm. There is little variation in the cutoff electric field as the voltage is increased 2.5 times. A field value of 1.48×10^5 V/cm was achieved before breakdown.

Another feature notable in Fig. 10 is the difference in slope of the two plots. Chronologically, the 44 kV test was run 15 days before the 107 kV test and over the interim period the sample was pulse tested essentially every day with gradually improving results. Larger macroscopic fields, and assuming no change in field enhancement correspondingly larger microscopic fields, were applied without encountering breakdown as testing progressed. It would appear that a decrease in the work function was occurring, probably as the result of cleaning the W surface by ion bombardment.

An attempt was made to improve the performance of AMC-9 by the use of a gridded-cup-type anode which might eliminate any anode initiated breakdown. The attempt was not successful because of failure of the

delicate grid under dc operating conditions.

Although the improvement in performance with sample AMC-9 had been substantial, it was felt that elimination of the preferential field enhancement at the sample edges would yield even better results. Consequently, the same sample was re-etched and installed as sample AMC-10. An anode of only 0.060 inch diameter was installed, replacing the 0.75 inch diameter one used with samples AMC-7 through -9. Direct current performance of this sample was not particularly good, and under pulse operation no current was observable even though the highest macroscopic fields, 2.13×10^5 V/cm, used in the course of this work were applied without encountering breakdown, When breakdown did occur, it was observed in the sample center rather than on the edge as in all previous instances. It would appear that preferential field enhancement occurred in the sample center, and that a somewhat larger diameter anode would be preferred.

Sample AMC-11 represented another approach to the problem of reducing the preferential emission from the sample edges. A sample with the "pot-hole" geometry shown in Fig. 11 was utilized theorizing that the pins near the edges of the "pot-holes" would act as edges, thereby providing a substantial edge length uniformly distributed across the sample surface. Pulse emission performance of the sample was as good as any achieved during the course of the program, but the hoped-for improvements were not evidenced. Post-emission scanning electron microscope inspection of the sample showed all emission related damage to have occurred on the sample edges as with all previous geometries utilizing large anodes. It is of interest to note that a

maximum field of 1.22×10^5 V/cm was applicable to this sample, but results comparable to AMC-9 were achieved at this lower field value.

C. Area Scalability

Sample AMC-4 initiated a series of tests intended to demonstrate the current versus area scalability of the emitters. A sample holder capable of holding up to three samples was designed and installed in the emission testing rig with sample AMC-4 initially, followed by the addition of sample AMC-5 and then AMC-6. This increased the emitter area from approximately 0.3 cm^2 to 0.9 cm^2. Standard operating conditions substantially below the breakdown threshold were established with sample AMC-4, specifically an interelectrode spacing of 0.125 inch and an applied potential of 23 kV. Under these conditions sample AMC-4 gave 2.0 mA of current; samples AMC-4 and -5 gave 4.0 mA; and samples AMC-4, -4, and -6 gave 6.0 mA. These results indicate that the current increases as a direct function of the area.

Scalability was not demonstrated up to a factor of ten because of voltage breakdown problems. It was decided to devote the major experimental effort to what was felt to be the more fundamental problem.

SECTION IV

The Effects of Electrode Design on Emission and Breakdown

The experimental results presented in the preceding section indicate that the cathode configuration and the density of the emitter pins are the keys to a successful gun design. It was observed that the difference between good emission current and no emission or breakdown was often only the height of the emitter above the cathode plane. In most cases when operation above about 110 kV was attempted, useful current could not be obtained before electrical breakdown occurred. Since many times the required current had been routinely obtained at lower voltages, it was unlikely that the emitter pins were operating at anywhere near their limiting currents. Because the only difference between low voltage and high voltage operation is the mounting arrangement and the interelectrode spacing involved, it became imporant to investigate in a systematic fashion how these factors influence the emission.

The initiation of field emission requires a local electric field of about 10^7-10^8 V/cm. This large electric field is derived by concentrating the macroscopic field (V/d) at the emitter pin tips. To a crude approximation, the field at the pin tips is the macroscopic (parallel plate) electric field multiplied by a field enhancement factor. Since the existence of field emission requires a field of approximately 10^8 V/cm and the macroscopic field is typically approximately 10^5 V/cm, the field enhancement factor is 100-1000. The pin-tip electric field is 100-1000 times larger than the value

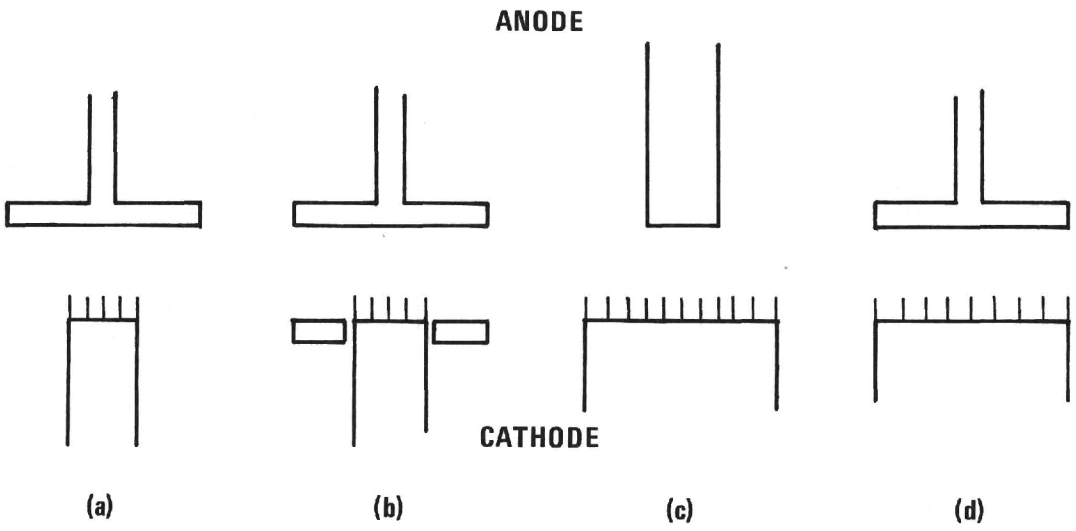

Figure 12. Possible Field Effect Diode Geometries.

determined simply by dividing the anode voltage by the interelectrode spacing. The field near the tips is affected by any change in the larger scale macroscopic field. Thus edge effects can be of considerable significance in reducing or increasing the pin-tip electric field. Edge effects are certainly macroscopic when viewed on the scale of the pin tips. Hence, to first approximation, the local electrical field is directly scaled by relative macroscopic edge effects or other field perturbations.

The effective field enhancement factor of an array of emitter pins is a function of the pin density. Since the pin density falls to zero at the emitter boundary, there is an effective lessening of the density as the edge is approached. Hence, the field enhancement factor changes near the edge of the emitter sample.

There are then two effects near the edge of an emitter wafer. The macroscopic electric field is changed because of edge effects and the effective field enhancement factor is changed with effective pin density. The emission current will thereby be affected strongly by the product of these two effects. Specific examples of the above effects are considered below.

Figure 12 shows several possible diode geometries. These different geometries were studied using a resistance paper analog to determine the edge effects present in each case. While not strictly valid, the resistance paper method provided a quick qualitative insight into the behavior of the several emitter configurations. The several geometries were outlined to the same scale using silver paint. A regulated power supply and a digital voltmeter were used to plot

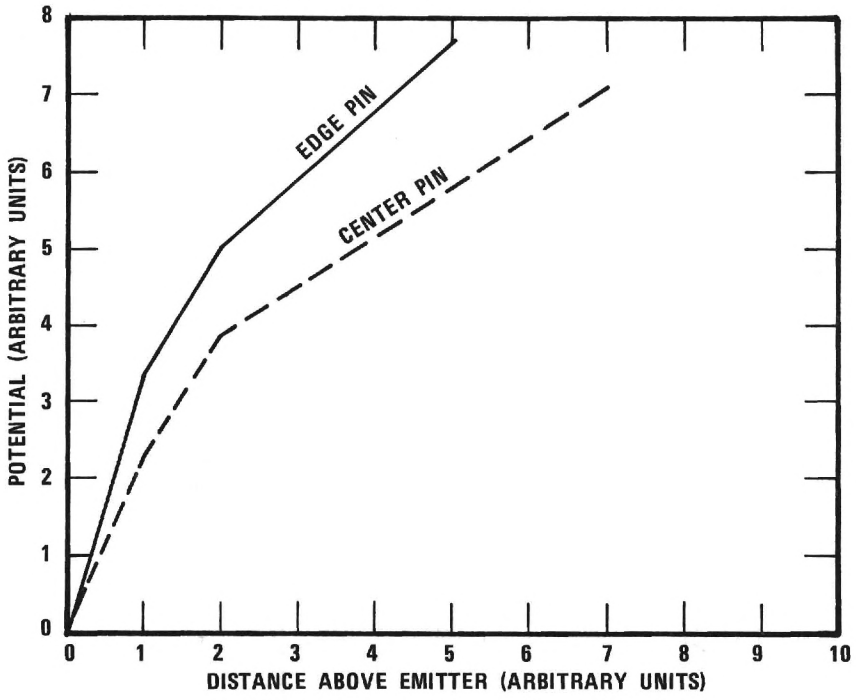

Figure 13. Potential Variation Above Edge Pin and Center Pin for Small Cathode--Large Anode. See Figure 12a.

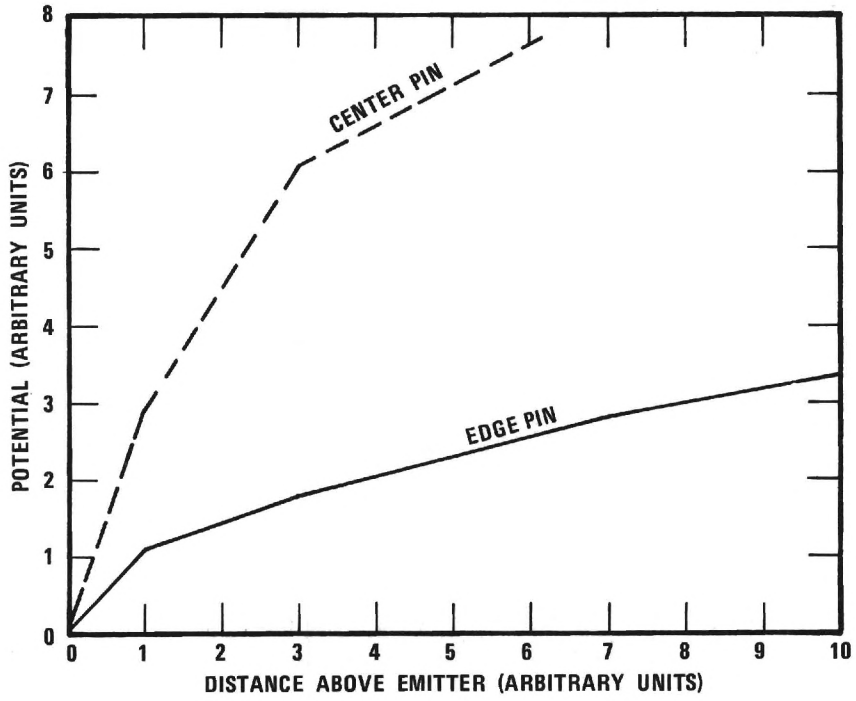

Figure 14. Potential Variation Above Edge Pin and Center Pin for Large Cathode--Small Anode. See Figure 12c.

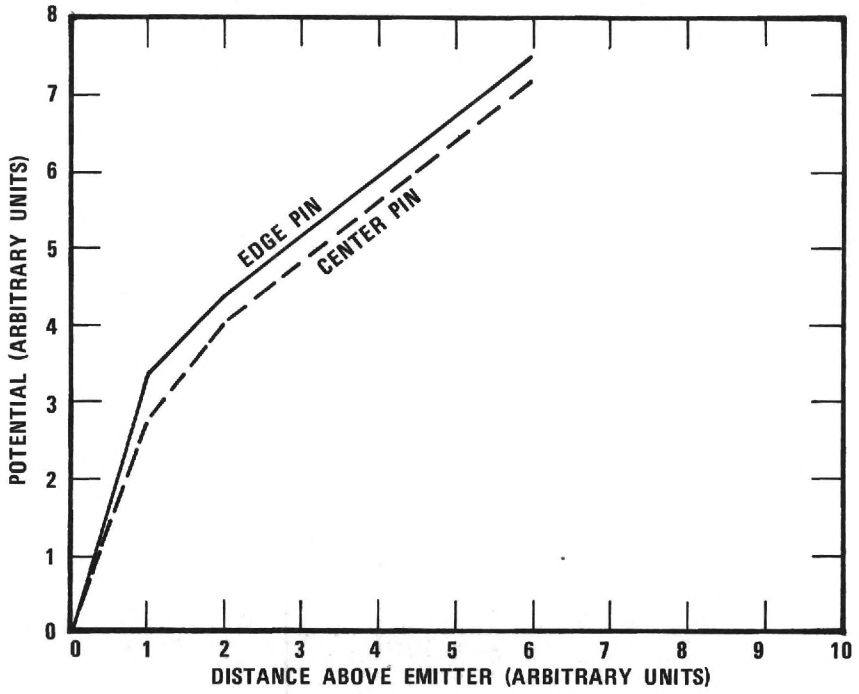

Figure 15. Potential Variation Above Edge Pin and Center Pin for Same Size Anode and Cathode. See Figure 12d.

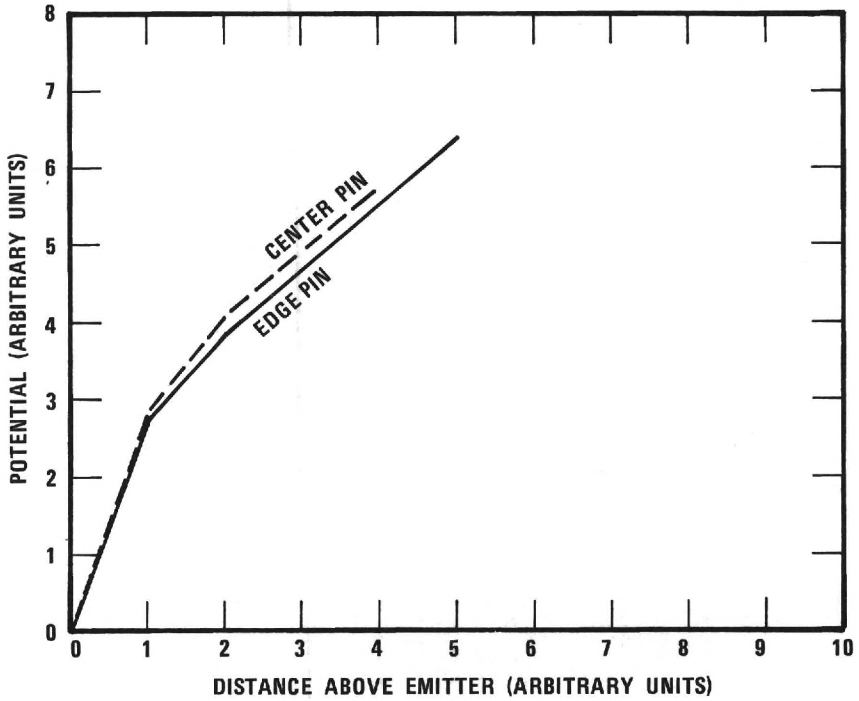

Figure 16. Potential Variation Above Edge Pin and Center Pin for Guarded Cathode. See Figure 12b.

equipotential lines. The results of these tests are given in Figs. 13 - 16. The figures show the variation in potential above a given pin along the pin axis. The slope of the curves is proportional to the electric field along the pin axis from the pin tip upward. Each graph considers two pins, one centrally located beneath the anode and the other at the edge of the cathode. The variation of the electric field at these two pins is a good measure of any edge effects. Figure 13 shows the data for the small-cathode-large-anode. This is the situation in the majority of early dc experimental work. It can be seen from the figure that the field is significantly stronger nearer the emitter edge than in the middle. This effect was seen to decrease with distance from the cathode edge. Hence, unless changed by packing density effects, this emitter configuration would result in greatly increased emission from pins on the edge of the emitter wafer.

Figure 16 shows the results for the same configuration shown in 13 except that now a guard ring has been added. The effect of the guard ring is seen to greatly decrease the edge effects. Additional studies as well as experimental evidence (Chapter III) showed guard ring placement to have a strong influence on the edge effect. Most of the pulsed emission data were taken with a guarded-cathode configuration.

Figure 15 shows the results for an unguarded emitter approximately the same size as its anode. This configuration is similar to that in Fig. 13, but with a reduced effect. The edge pins are favored, but not as strongly as when the cathode is much smaller than the anode. Very few tests of either type were run with this diode configuration.

Figure 14 shows a configuration that was used to eliminate the edge-increased electric field. It is noted that the electric field at the tip of an interior pin is approximately four times that of an edge pin. This would result in enhanced emission from the central portion of the emitter wafer unless modified by packing density effects. A high current dc emission test sample using this configuration provided 1 A/cm^2 for 400 hours with no damage to the emitter.

As stated previously, the net effect on emission depends on the product of the macroscopic edge effect and the packing density effect. The packing density effects will now be considered. Any treatment of the packing density requires a suitable theory connecting field enhancement factor with the pin radius and other parameters. Two approaches will be used which have been both reported in our previous work. Consider first a two dimensional approximation.[1,3] In this approximation the emitter is assumed to be in the form of a two dimensional array. Each individual hemispherical emitter has a radius R and is spaced on a grid of size a. Other parameters are the interelectrode spacing L and the interelectrode voltage V. This technique predicts the macroscopic emission current density to be:

$$J = B \frac{\pi R^2}{a^2} \left(\frac{V}{R}\right)^2 \frac{1}{1 + 4\pi \frac{RL}{a^2}} \; e^{R\left(1 + \pi \frac{RL}{a^2}\right)\frac{F_R}{V}}$$

where B and F_R are constants.

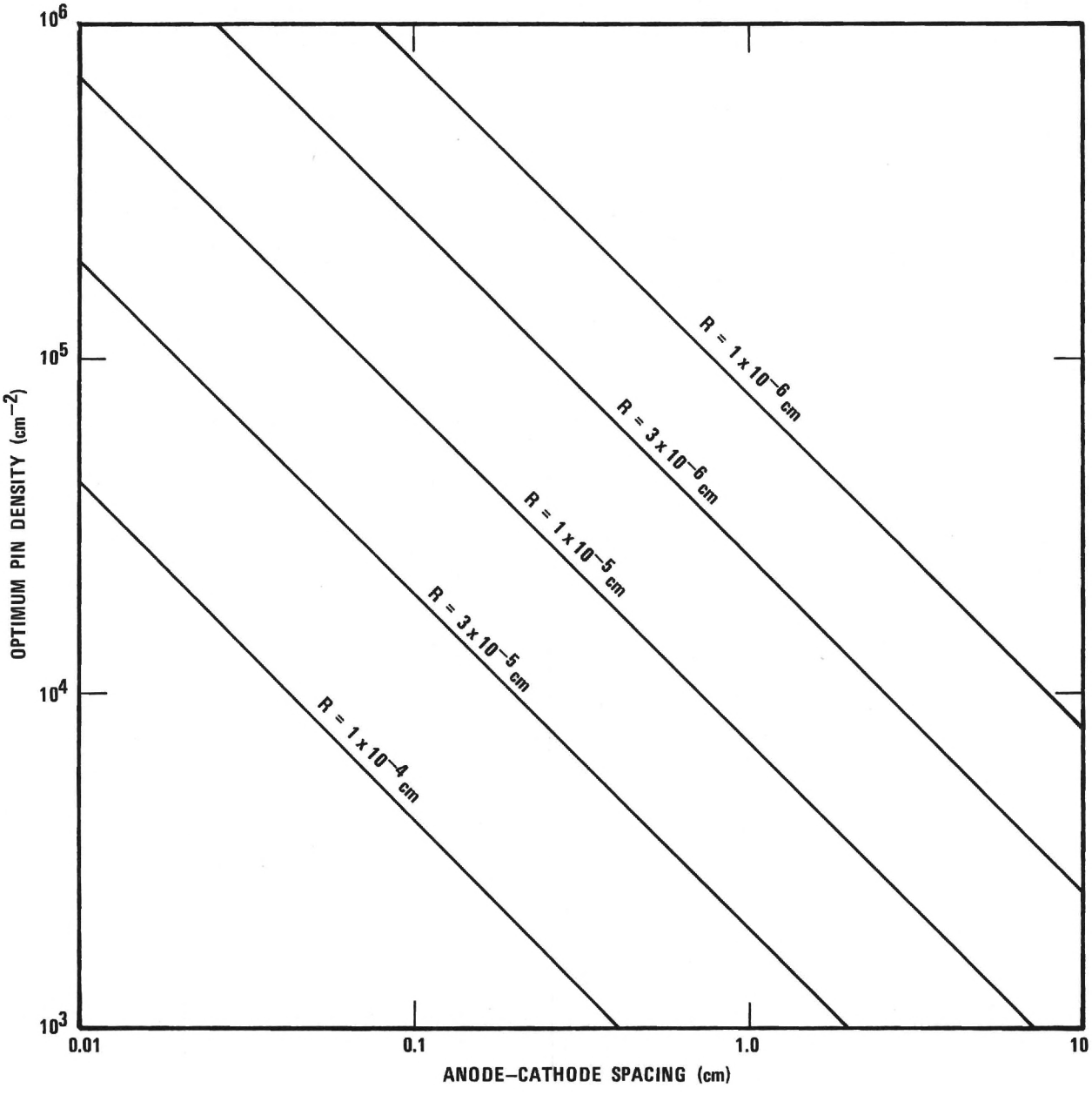

Figure 17. Optimum Pin Density as a Function of Interelectrode Spacing with Pin Radius as a Parameter.

The optimum a is obtained from the above equation to be:

$$a_{opt} = \left\{2\pi RL\left[\left(1+R\frac{F_R}{V}\right) + \sqrt{1+6R\frac{F_R}{V}+R^2\frac{F_R^2}{V^2}}\right]\right\}^{\frac{1}{2}}$$

For large V,

$$a_{opt} \cong \sqrt{4\pi RL} = 2\sqrt{\pi RL}$$

OR the optimum density $\frac{1}{a^2} = D$

$$\frac{1}{a_{opt}^2} = \frac{1}{4\pi RL}$$

$$D_{opt} = \frac{1}{4\pi RL}$$

A plot of the optimum density as a function of interelectrode spacing with pin tip radius as a parameter is given in Fig. 17.

This equation is of considerable importance in the present work. It indicates that the optimum density is significantly smaller than that accessible to the growth technique and becomes even more inaccessible as the interelectrode spacing is increased. Under such conditions, one would expect the effective density decrease as the edge is approached to always result in an increase in emission current. Hence, an edge effect leading to a still higher relative emission from the outer edge pins. At larger anode-cathode spacings the macroscopic edge effects will not be as great, hence the electric field available for enhancement at the pin tips would be reduced. This coupled with the requirements for smaller pin densities with increased gap spacing could lead to a reduced

emitter efficiency with increased interelectrode gap. That is, scaling the voltage and gap together would not result in constant emission current. Unfortunately, this prediction is to some extent observed.

A second, more rigorous treatment of the field emission from arrays was based upon a combination of numerical and analytical approximations.[4] These results which are not in a convenient form for comparisons also suggest that the optimum pin density is considerably lower than those which have been used. The above conclusions concerning the behavior of the outer edge pins are thus reinforced by the second theory.

SECTION V

Prototype Fabrication of Large Area Array

Operational electron beam lasers will require cathodes many times larger than those tested in this program. The maximum size emitter that can be produced by existing unidirectional solidification technology has about 12 mm of usable diameter. Consequently, electron beam lasers will require an array of emitter wafers. A 10×100 cm array is a useful prototype size. Such an array will use fabrication techniques developed in the present and previous work. It is proposed to use round wafer-shaped cathodes, approximately 12 mm in diameter, copper brazed to a smaller diameter molybdenum rod and arranged in a square array. Using this configuration, a rectangle containing 8×84 individual emitters would be required. Without going into all of the composite growth and fabrication steps required to make the individual emitters needed to construct the large array, a reasonable estimate of the fabrication cost is between $40 and $60 per individual emitter. Since the square array would use almost 700 such cathode structures, the approximate cost is between $30,000 and $40,000 for this design.

This proposed design has some major advantages over any attempt to make a continuous flat mosaic of this size. Should individual emitters not perform well, they could be replaced separately without disturbing the remaining array. It is anticipated that the small amount of void area between the individual wafers would not adversely affect the electron density in the laser gas because of the scattering expected

through the foil. If needed, a modest increase in emitter area could be achieved by placing the individual wafers to form a hexagonal array. This design could be expected to yield microsecond pulses of 10-20 mA/cm^2 across the total 1000 cm^2 area.

A continuing effort is presently underway to improve the emitter configurations and/or diode designs, and the size of the unidirectionally solidified composite ingots. Any advances in these areas will decrease the estimated cost to fabricate any large area cathode structure.

SECTION VI

Conclusions and Recommendations

On the basis of the work outlined in the preceding section, it is concluded that the oxide-metal field effect electron emitters will not at the present time meet the design criteria for gas laser electron guns, but could meet those criteria if the problem of high voltage breakdown were solved. It is recommended that a program devoted only to this problem be considered for implementation.

The performance of the oxide-metal field effect electron emitters in relation to the design goals is summarized in Table II below.

TABLE II. Comparison of Performance with Design Goals.

Parameter	Target	Demonstrated
Current Density	100 mA/cm^2 @ 150 kV	130 mA/cm^2 @ 107 kV
Maximum Current	300 mA	38 mA
Maximum Voltage	150 kV	120 kV
Maximum Area	3.0 cm^2	1.0 cm^2
Area Scalability	$\times$ 10	$\times$ 3

Although the demonstrated results are below the target values in all categories except maximum current density, it is felt that only the voltage limitation is significant. Area scalability by a factor of three was demonstrated with no difficulty. Further increases in emission area were not attempted as efforts were devoted to the voltage breakdown

problem. However, it is believed that if care is taken in the emitter wafer mounting, the total current could be scaled to almost any desired value.

Since the emitters have demonstrated more than 1 A/cm^2 at lower (< 5 kV) operating voltage, it is very unlikely that the required emission current is limited by failure of the emitter pins. It is concluded that the failure to achieve the desired operating voltage level is the result of the field enhancement factor decay with increasing spacing coupled with a non-optimum electrode design. It is believed that techniques which reduce the emitting pin density, when used with better electrode design would result in a substantial improvement in performance.

Several methods exist by which considerable improvement in emission performance might be obtained. These approaches involve adjusting the emitter pin density, optimizing the electrode design, and using resistively loaded emitters.

Growth techniques have been perfected which indicate that a pin density of several million per cm^2 is now feasible. The apparent density can be further slightly reduced by etching the pins in the form of long tapered spikes. However, it is likely that the density will still be larger than desired. A mechanical technique whereby rows of pins are removed might be feasible. Prototype fabrication could be accomplished with a micromanipulator in the scanning electron microscope. Production runs might rely on photochemical etching methods.

It is possible that the electrode design might be improved to provide a larger field before breakdown occurs while limiting

preferential edge emission from the wafers. The Rogowski technique has long been used to eliminate edge effects in electrode design. However, the Rogowski[5] method encounters several obstacles when applied to the field emitter geometry. First, the Rogowski electrode shape is valid for only one interelectrode spacing. This constraint would not be important unless a variable spacing were desired. A more important consideration is that the curvature of the electrodes is of the same order of size as the interelectrode gap. In fact, the extent of the electrode contour is usually larger than the gap. Thus, the emitter will have to be mounted in such a fashion that the difficulties outlined in Chapter IV are not encountered. In addition, the large area required by the electrode design will necessitate an increased emission density from the wafer to maintain the same overall current.

Previous experiments have shown that field emission current stability and emitter lifetime could be enhanced if a large series resistance were placed in the diode circuit. The resistance introduced stablizing negative feedback by reducing the interelectrode voltage upon an increase in current. The ideal situation would be to have a resistance in series with each emitter pin. Such a resistance would confine its effect to a single pin and would not significantly affect the overall emission. Another potential advantage of individual pin resistances is the reduction of edge effects. Mounting geometries discussed in Chapter IV combined with pin density effects produce increased emission as the emitter edge is approached. Individual pin series resistances could be used to compensate for these effects. Figure 18 shows an emitter designed to reduce edge effects by exploiting

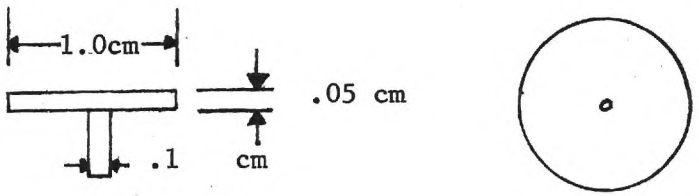

Figure 18. Resistively Loaded Emitter.

the resistive properties of the UO_2 matrix. A small metal pin is brazed to the center of an emitter disk. Current emitted from pins near the periphery of the disk produce considerable voltage drop across the material. Hence, to first order, the interelectrode voltage is reduced and the outer pins are prevented from dominating the emission. Figure 19 shows the theoretical performance of such a system. The curves give the interelectrode voltage across the emitter with the voltage at the outer emitter edge as a parameter. Note that to maintain 1000 V at the emitter edge requires only a few volts more on the center pin, while maintaining 1500 V at the emitter edge requires 2170 V on the center pin. This indicates, in principle, the effect possible with this scheme.

Finally, a newly developed concept in the oxide-metal composite field emitter area provides an attractive alternative, allowing production of an electron beam at an applied potential of 100 volts or less. The low voltage emitter arrays are produced by first argon-ion milling the composite. The milling produces conical depressions centered on each emitter pin with the pin at each apex. An insulating layer (SiO_2)

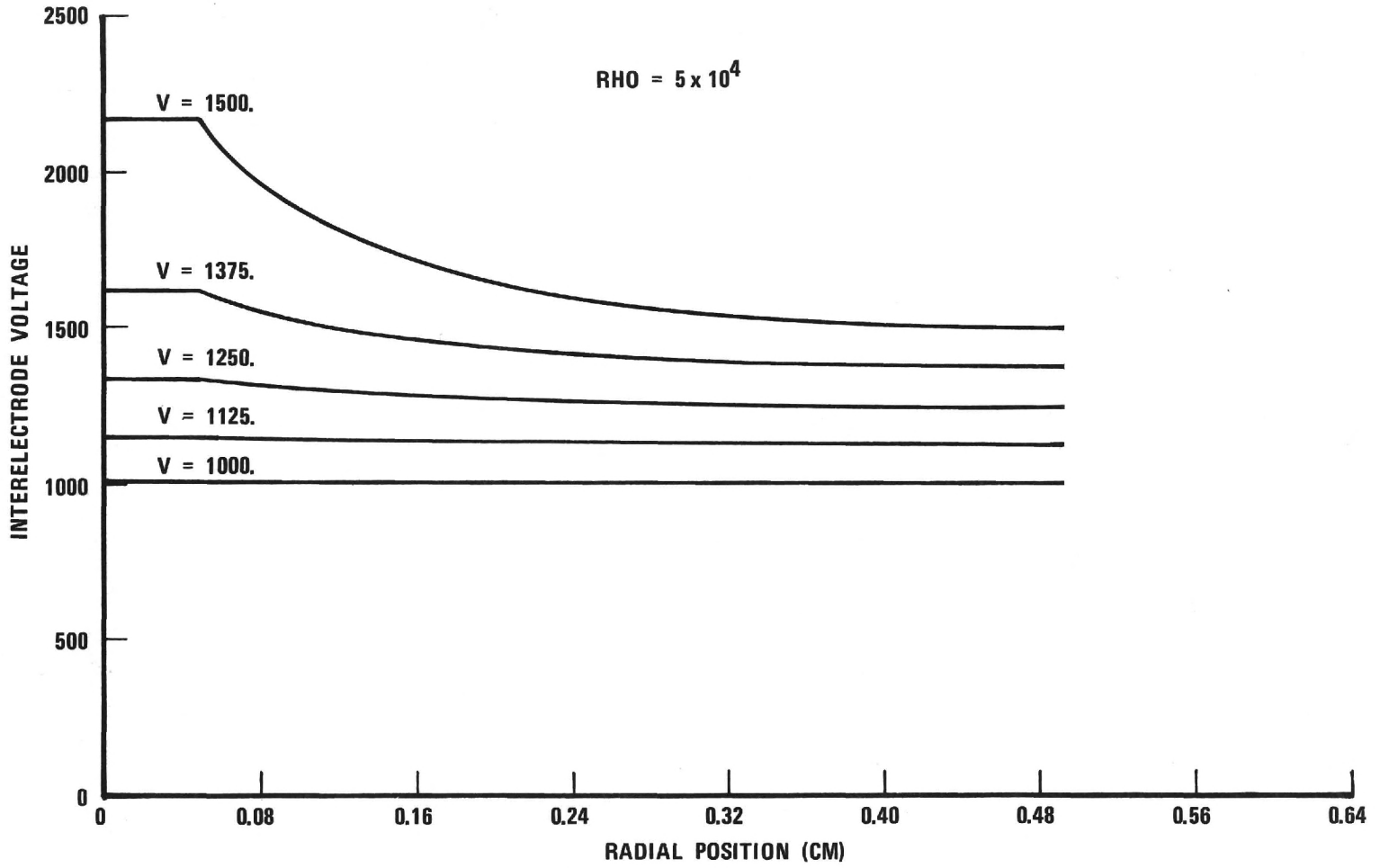

Figure 19. Interelectrode Voltage Variation Across Resistively Loaded Emitter. Wafer Thickness 0.05 cm; Wafer Diameter, 1.0 cm; Support Diameter, 0.1 cm; Resistivity, 5×10^4 ohm-cm.

and a conducting layer (Co) are then sequentially vapor deposited at a low angle while the sample is rotating. Figures 20 and 21 give, respectively, sketches and a photomicrograph of the emitter arrays. Very preliminary testing has produced emission current densities of about 50 μA with less than 100 V applied between the pins and the anode layer.

Considering the simplifications possible when 100 V or less pulses can be used to produce the electron beam, followed by acceleration to the required potential, this geometry may provide the most attractive solution. It is recommended that a program to examine low voltage emitters for the gas laser application be considered, possibly in conjunction with an investigation of the previously discussed breakdown prevention techniques.

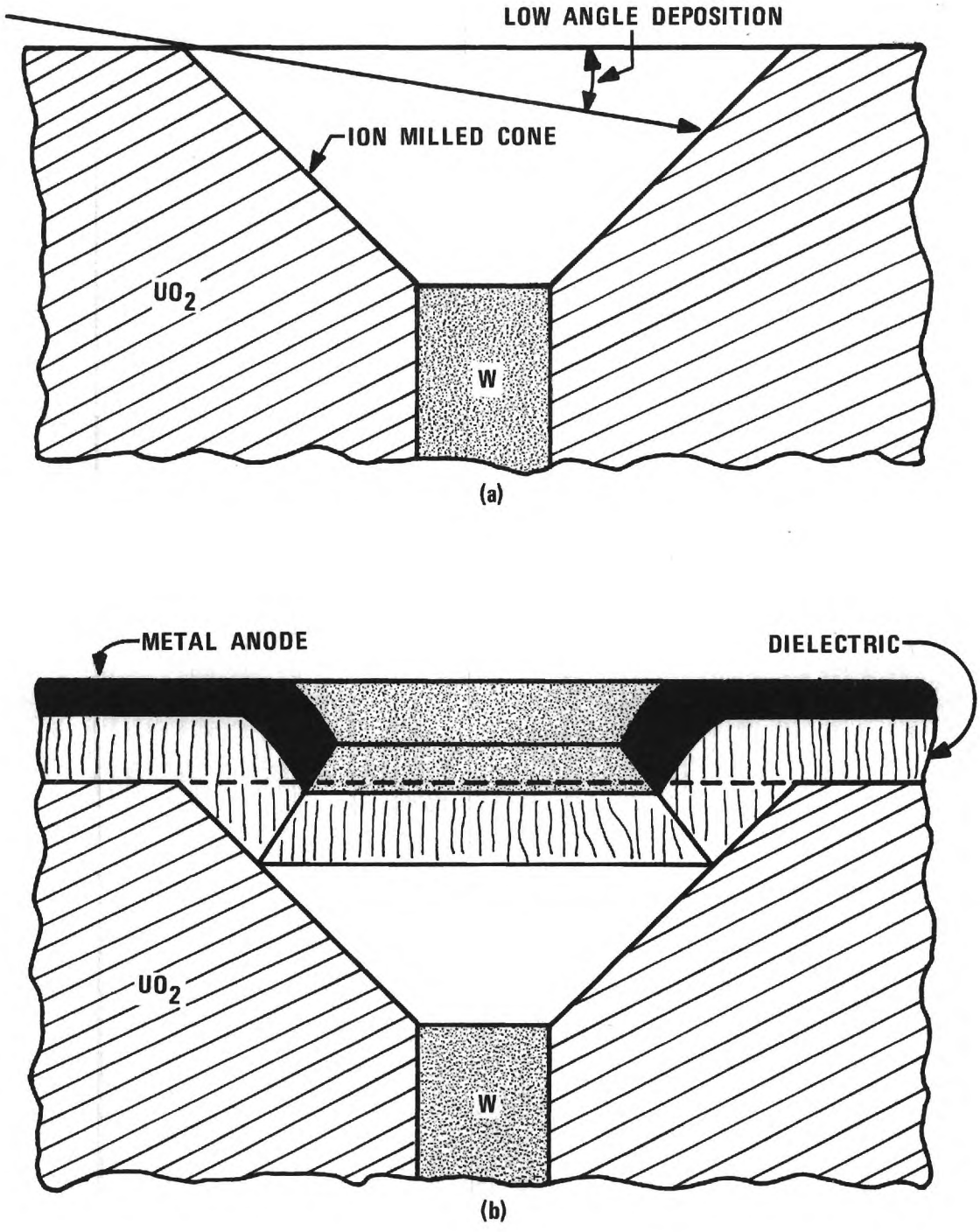

Figure 20. Schematics of (a) Cones Produced in UO_2-W Composites by Argon Ion Milling and (b) Low Voltage Emitter Structures After Sequential Low Angle Deposition of a Dielectric and a Metal on a Rotating Ion Milled Composite.

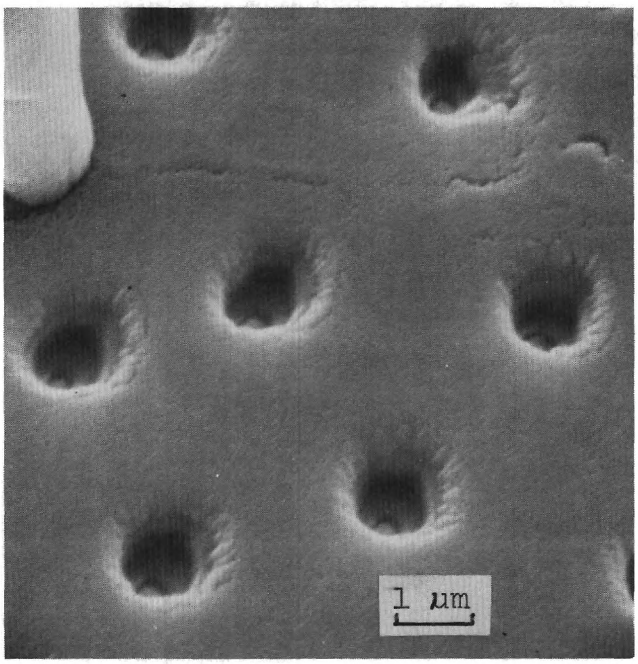

Figure 21. Scanning Electron Micrograph of Completed Electron Gun Array.

REFERENCES

1. A. T. Chapman, et al., "Melt-Grown Oxide-Metal Composites," Report No. 2, Final Technical Report, ARPA Contract DAAH01-70-C-1157 and ARPA Order No. 1637, School of Ceramic Engineering, Georgia Institute of Technology, July 1971.

2. A. T. Chapman, et al., "Melt-Grown Oxide-Metal Composites," Report No. 4, Annual Technical Report, ARPA Contract DAAH01-71-C-1046 and ARPA Order No. 1637, School of Ceramic Engineering, Georgia Institute of Technology, July 1972.

3. J. D. Levine, RCA Rev. 32, 144 (1971).

4. A. T. Chapman et al., "Melt-Grown Oxide-Metal Composites," Report No. 6, Final Technical Report, ARPA Contract DAAH01-71-C-1046 and ARPA Order No. 1637, School of Ceramic Engineering, Georgia Institute of Technology, December 1973.

5. J. D. Cobine, Gaseous Conductors, Dover, N.Y., pp. 177, 180.